

PL/PA 16 DEC 96

## Sensor and Simulation Notes

Note 187

DETERMINATION OF THE IN SITU GROUND CONDUCTIVITY  
AND RELATIVE DIELECTRIC CONSTANT VIA THE TWO-LOOP  
METHOD USING SWEEPED FREQUENCY EXCITATIONJeff Lytle  
Ed Laine  
Darrel LagerLawrence Livermore Laboratory  
Livermore, California

August 8, 1972

## Abstract

A technique is described which is an easy method for determining the in situ ground conductivity  $\sigma$  and relative dielectric constant  $\epsilon_r$ . Particular emphasis has been concentrated on numerical calculations and experimental equipment in the 0.1- to 21-MHz frequency range. The governing formulae and consequent numerical results are given which illustrate the effect of both a uniform and a vertically stratified ground upon swept-frequency, two-loop mutual impedance measurements. The effectiveness of overburden thickness and conductivity on masking the subsurface ground conductivity as measured using a two-loop mutual impedance procedure is illustrated. Conductivities of  $10^{-4}$  to  $2 \times 10^{-1}$  mho/m and relative dielectric constants of 5 to 25 are considered in the numerical evaluations.

PL 96-0990

01 01 0000

## Contents

Abstract . . . . .	1
Introduction . . . . .	3
The Measurement Procedure - A Ratio Method . . . . .	6
Experimental System . . . . .	9
Mathematical Representations . . . . .	14
Numerical Results . . . . .	18
Homogeneous Media . . . . .	18
Stratified Media . . . . .	21
Validity of Approximate Formulae . . . . .	25
Additional Comments . . . . .	26
Conclusions . . . . .	46
Acknowledgements . . . . .	70
References . . . . .	70

## Introduction

A variety of methods are available for determining the local constitutive parameters (conductivity  $\sigma$  and relative dielectric constant  $\epsilon_r$ ) of the ground. Some examples <sup>1</sup> are measurements of the wave tilt of signals from a distant transmitter, the use of four-probe arrays (e.g., Eltran, Wenner, right angle, etc.), and the use of mutual impedance measurements on two loops. This report is concerned with a two-loop swept-frequency experimental system developed and used by Lawrence Livermore Laboratory (LLL). No attempt will be made to present results for the four-probe, wave tilt, or alternate methods.

The two-loop method has been extensively used in ground conductivity surveys and in geophysical prospecting. A large percentage of work has been for frequencies  $<1$  MHz where earth conduction currents typically dominate earth displacement currents, i.e.,  $\sigma \gg \omega \epsilon_0 \epsilon_r$ .

The basic theory of loop antennae over a conducting earth was originally presented by Sommerfeld <sup>2</sup> in 1909. It was not until the work of Wait <sup>3-5</sup> in the 1950's, however, that a formulation of the theory was presented upon which calculations for practical interpretation of data could be based. Wait has considered both a homogeneous half space and layered stratified ground cases. Keller and Frischknecht <sup>1</sup> and Jöhler <sup>6</sup> have presented numerical results for a homogeneous half space. Barrows <sup>7</sup> has extended the procedure by developing a computer program which accounts for stratified ground. Recent investigations <sup>6-9</sup> have included the effect of both conduction and displacement currents.

The stratified ground situation is interesting because of a number of experimental sites, the ground may not be uniform or homogeneous. An example is a surface layer of high conductivity. Another example is a ground in which the conductivity either increases or decreases with depth. These types of ground naturally lead to different experimental results than one would obtain for a homogeneous ground.

There has been an increase in the use of the two-loop method in recent years, and some work has been performed using a pulse-loop excitation <sup>1,10</sup> rather than selected cw frequencies. Much emphasis using pulse techniques has been in the quasistatic regime, i.e., distances small compared to the free space wavelength. This typically requires use of frequencies < MHz for normal loop separations.

The authors are not familiar with any documentation regarding use of swept frequency techniques in conjunction with the two-loop system to determine the ground constitutive parameters, although it is a rather simple extension of the selected cw frequency approach. This report presents illustrative results which one can expect using a swept frequency technique for  $0.1 \leq f \leq 21$  MHz for a wide variety of ground conditions. The results which one can expect are of course also valid for selected cw frequencies in this frequency range. We have found that if one is interested in a particular site, the sweep procedure yields more data much more quickly and easily than does sampling a variety of cw frequencies. We believe it yields as much information as a pulse technique. In addition, it overcomes a practical detail, namely, the need for a relatively high-power, wide-band balun for detailed reduction of pulse excitation data.

For airplane surveys of a ground anomalies , the pulse excitation system yields more useful data than a swept frequency system because of restrictions placed on the sweep rate by the airplane speed. For surveys at a particular site to determine ground conductivity rather than geophysical prospecting or detection of ground anomalies, we believe that the swept frequency system is better than either a selected cw or a pulse system because of the relative ease of measurement, the relative time required for each measurement, and the rapid data reduction capability.

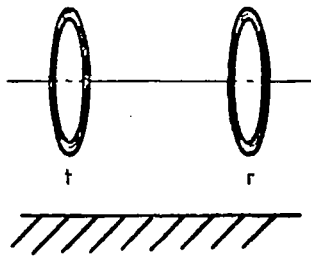
A ratio technique is proposed for use with the swept system. This eliminates any uncertainties in the transmitted signal, whereas an absolute measurement of induced receiving loop voltages is dependent upon transmitting loop uncertainties.

#### THE MEASUREMENT PROCEDURE - A RATIO METHOD

For two loops - a transmitter and a receiver - located at the same height above ground, three orientations of transmitter and receiver are readily amenable to mathematical analysis and modeling. These are indicated in Figure 1 and consist of the possible combinations of horizontal and vertical loop antennae. Arbitrarily oriented loops could also be used, but their consideration would greatly increase the numerical results one would need to calculate. To eliminate this difficulty, we will only consider the three combinations shown in Figure 1. Following the now standard notation<sup>1</sup> these cases are denoted as the coaxial, perpendicular and coplanar cases.

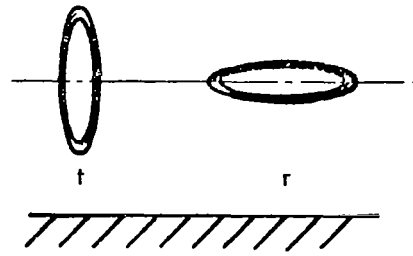
In the theoretical model, the transmitter loop is represented as a single magnetic dipole. This means that an effectively uniform current distribution about the experimental loop antenna is required or that the circumference of the loop be  $< \lambda/5$ . Separation distances between loops of more than five times the loop diameters are also required for a valid theoretical model. Hence, the physical dimensions of the loops dictate the high-frequency limit for a valid comparison of the simple theory and the equipment.

The following ratio procedure is proposed because it eliminates or helps to eliminate many of the difficulties inherent in an experimental procedure based on absolute measurements. Two cases are considered, the coaxial/perpendicular and the coplanar/perpendicular. In the coaxial/perpendicular case, the plane of the transmitter loop is oriented vertically (see Figures 1a and 1b). The induced voltage is measured as a function of frequency for two orientations of the receiver loop plane, vertical (Figure 1a) and horizontal (Figure 1b). The ratio of the voltage magnitudes (in dB) and their phase difference are thus obtained for the coaxial/perpendicular case. In the coplanar/perpendicular case (see Figures 1c and 1d), the transmitter loop plane is oriented horizontally. The comparisons between horizontal and vertical receiver loop orientations are repeated. The ratio of the voltage magnitudes (in dB) and their phase difference are thus obtained for the coplanar/perpendicular case.



Coaxial

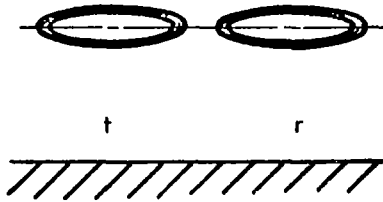
(A)



Perpendicular

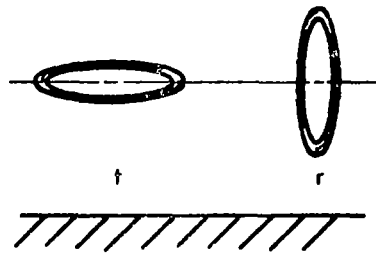
(B)

Horizontal magnetic dipole transmitter cases



Coplanar

(C)



Perpendicular

(D)

Vertical magnetic dipole transmitter cases

---

Fig. 1. Various loop orientations.

An alternate method for determining the ground conductivity and relative dielectric constant mutual impedance for a particular orientation rather than the ratio measurement described above. Experimental systems using absolute measurements have been tested and used by others <sup>6,8</sup> in field tests at a number of sites. Numerical results are presented herein for both the absolute mutual impedance and the ratio of mutual impedances.

#### EXPERIMENTAL SYSTEM

The two-loop experiment system is shown in block diagram form in Figure 2. A linear sweep generator output is coupled to the wide-band power amplifier, giving 5 W from 250kHz to 110 MHz. The output of the wide-band transformer. The sweep generator is also coupled to a network analyzer. This provides a voltage-tunable oscillator (VTO) output to operate the tracking detector. It also provides blanking and horizontally synchronized sweep voltage to the CRT display.

The network analyzer has two inputs--one a reference voltage, the other the signal or test voltage. The network analyzer will accurately measure the amplitude and phase difference between these two voltages on a swept basis. The reference signal is held constant within the instrument and the test signal is compared to it. Maximum sensitivity is -10 to -90 dBm.

The reference and test loops are identical in physical construction, but the test loop requires a preamplifier. The reference loop is

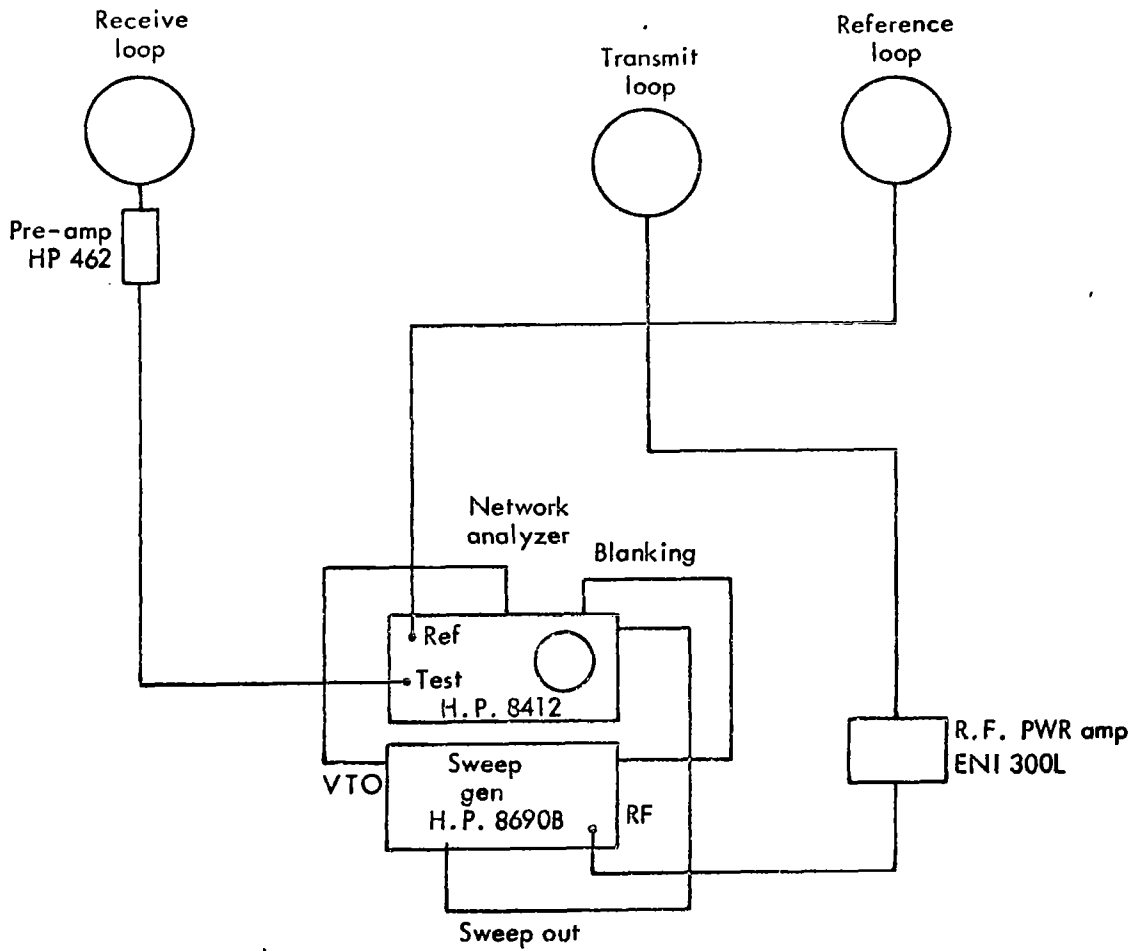


Fig. 2. Block diagram—swept-frequency, two-loop system.

placed closer to the transmitting loop. Because a measured ratio is used instead of an absolute value and because the system is independent of the transmitter loop and its power variations, quite good accuracies can be expected on a swept basis.

The loops are typically positioned with a 5- or 10-m separation between the transmitter and test loop. The power is adjusted until the reference loop output remains within the boundaries of the reference indicator level for the frequencies of interest. A polaroid photograph records the magnitude and phase display while the test loop is coaxial with the transmitter loop (see Figure 1). The test loop is then rotated 90 degrees and another sweep is made on the same photograph. This photograph will now show four traces; i.e., both phase and amplitude at 0 deg orientation (coaxial) and at 90 deg (perpendicular) over the entire spectrum selected on the sweep generator. (Experimental results for a homogeneous ground should be similar to the numerical results depicted in Figures 5 - 10, explained later in this report, for the coaxial/perpendicular situation.)

Figure 3 shows the construction of the receiving (test) and reference loops. It was found that this type of loop gave the best balance. One can quickly check the balance by making one photograph of four sweeps with the test loop positioned at 0, 90, 180 and 270 deg. The 0 and 180 deg cases should be identical in magnitude and 180 deg out of phase. The same should hold for the 90 and 270 deg cases.

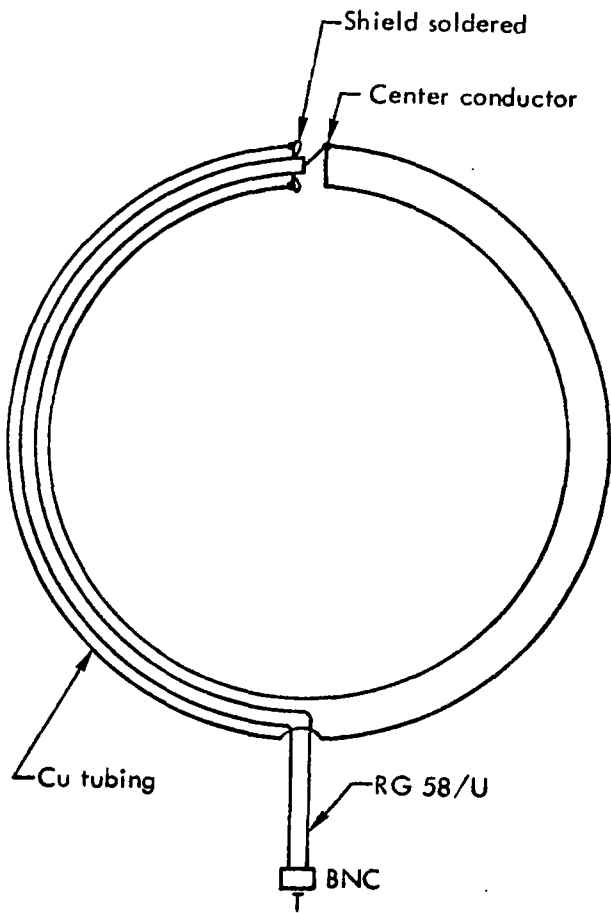


Fig. 3. Receiving reference loop construction.

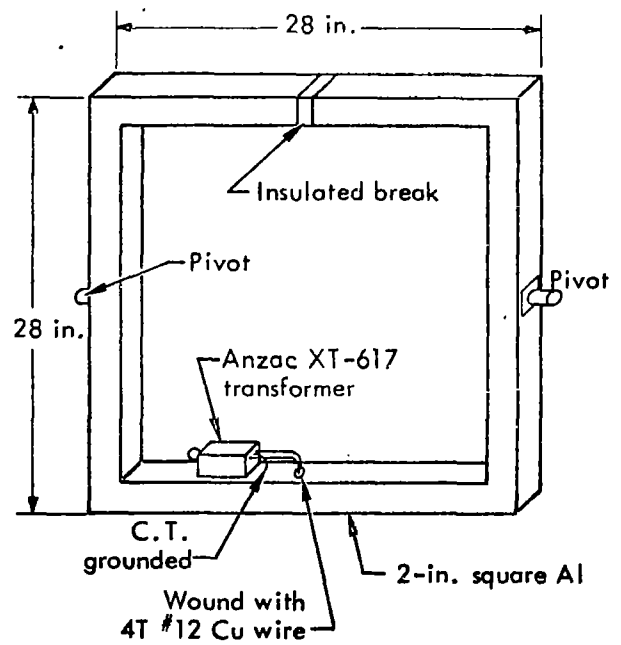


Fig. 4. Transmitter loop construction.

At the time of these experiments, a rather inefficient transmitter loop was in use\*. Plans call for the development of a wide-band loop capable of handling 10 W of power over the frequency range of 100 kHz to 21 MHz. The receiving loop works well into 50Ω because the loop impedance is low. This is not true in the case of a transmitting loop, so the problems are different. Figure 4 illustrates the construction of the present four-turn transmitter loop.

\*NOTE: While this report was being processed, an improved experimental procedure was developed. It uses a pair of orthogonal loops as the receiving antennae. The ratio (in dB) of the output signals from the two receiving loops is displayed on the network analyzer scope trace. This eliminates the laborious task of determining the ratio (in dB) of the two signals by subtracting one scope from the other.

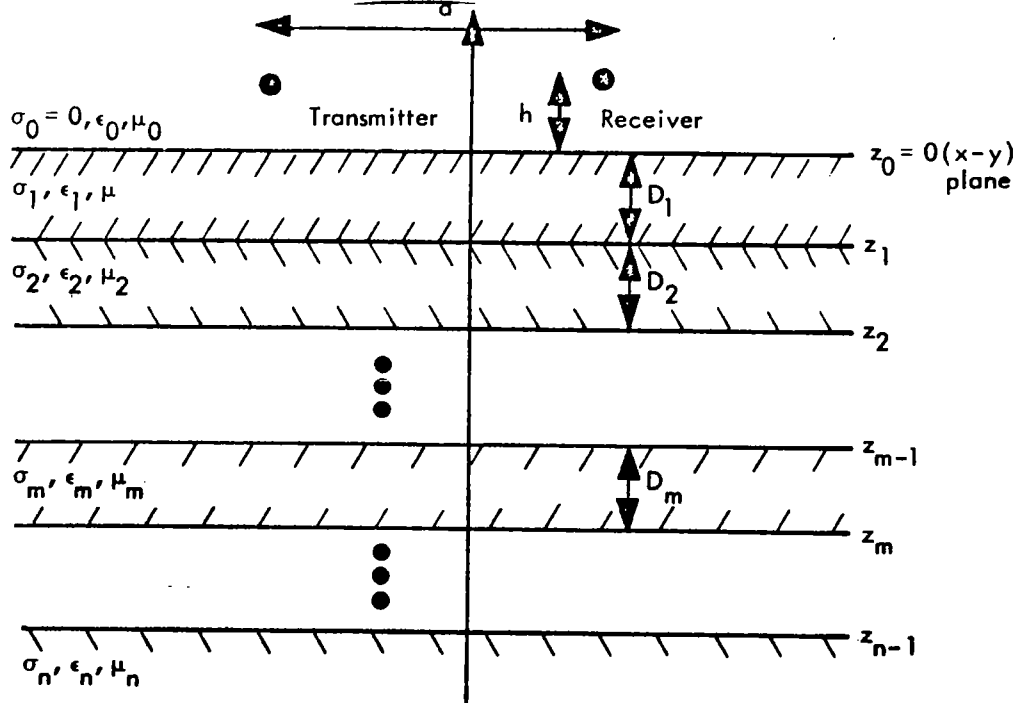


Fig. 5. A stratified media of  $N + 1$  layers.

## MATHEMATICAL REPRESENTATIONS

This section presents the formulas which have been used to compute the coaxial, coplanar, and perpendicular orientation mutual impedance. Two coplanar loops separated by a horizontal distance  $d$  have a mutual impedance in free space of

$$Z_0 = \frac{+j\omega N_1 N_2 A_1 A_2 10^{-7}}{d^3}$$

where  $A_1$ ,  $N_1$ ,  $A_2$ , and  $N_2$  are the area and number of turns, respectively, for loops 1 and 2. This formula enables one to express succinctly the mutual impedance for the coaxial, coplanar, and perpendicular cases in the vicinity of the earth. In all numerical work, it has been assumed that  $A_1 = A_2 = 1\text{m}^2$  and  $N_1 = N_2 = 1$ . The two loops are assumed to be at the same height  $h$  above ground and separated horizontally by a distance  $d$ . The formulas for the mutual impedance follow. The results are first presented for a homogeneous ground, and the modifications required for a stratified ground are then discussed.

Perpendicular:

$$Z = Z_0 d^3 \int_0^\infty \lambda^2 J_1 R_E e^{-2\gamma_0 h} d\lambda$$

Coplanar:

$$Z = Z_0 - Z_0 d^3 \int_0^\infty \lambda^3 J_0 R_E \frac{e^{-2\gamma_0 h}}{\gamma_0} d\lambda$$

Coaxial:

$$Z = -2Z_0 + Z_0 d^3 \int_0^{\infty} e^{-2\gamma_0 h} \times \left\{ \left[ J_0 - \frac{\lambda^3}{\gamma_0} R_M - \lambda \gamma_0 R_M - \lambda \gamma_0 R_E + k_0^2 R_M \right] + \frac{J_1}{d} \left[ \frac{\lambda^2}{\gamma_0} R_M + \gamma_0 R_M + \gamma_0 R_E \right] \right\} d\lambda$$

In the above formulas,

$$R_E = \frac{\gamma_0 - \gamma_1}{\gamma_0 + \gamma_1}, \quad R_M = \frac{k_0^2/\gamma_0 - k_1^2/\gamma_1}{k_0^2/\gamma_0 + k_1^2/\gamma_1},$$

$$\gamma_1^2 = \lambda^2 - k_{\text{ground}}^2, \quad \gamma_0^2 = \lambda^2 - k_{\text{air}}^2,$$

$$k_{\text{ground}}^2 = \omega^2 \mu_0 \epsilon_0 \epsilon_r - j\omega \mu_0 \sigma,$$

$$k_{\text{air}}^2 = \omega^2 \mu_0 \epsilon_0,$$

where  $\sigma$  and  $\epsilon_r$  are the conductivity and relative dielectric constant of the ground and  $J_0$  and  $J_1$  are cylindrical Bessel functions of order zero and one, respectively, where the argument of the Bessel functions is  $\lambda d$ .

It is noted that both conduction currents ( $\propto \sigma$ ) and displacement currents ( $\propto \omega \epsilon_0 \epsilon_r$ ) have been considered in this mathematical model. No approximations have been made, not even the usual quasistatic one where  $k_{\text{air}} = 0$ . These mutual impedance formulas have been evaluated using an accurate (albeit brute force) numerical quadrature algorithm (Romberg integration). Typical numerical results are presented later in this report.

As mentioned earlier, an experimental situation one might encounter is that of using the two-loop system over a vertically stratified ground. A pictorial representation of such a medium is shown in Figure 5. The upper region 0 is assumed to be air, and the ground surface layers are described by the dielectric constants  $\epsilon_m$  and conductivities  $\sigma_m$ . The thickness of the  $m$ th ground layer is assumed to be  $d_m$ . For convenience, it has been assumed that the permeability of each layer is  $\mu_0$ , or that of free space.

The coplanar, coaxial and perpendicular orientations are readily amenable to mathematical analysis for such a generally vertically stratified ground. Sparing the reader the mathematical details, we can easily show that the mutual impedance formulas (for the perpendicular, coaxial and coplanar orientations) for a stratified ground are the same form as for these orientations over a homogeneous ground. All that is required is use of the stratified ground reflection coefficients  $R^M$  and  $R^E$  in place of the homogeneous ground reflection coefficients  $R^M$  and  $R^E$  in the homogeneous ground formulas defined above.

How one determines the stratified media reflection coefficients  $R^E$  and  $R^M$  is explained below. The procedure is well known and has been previously applied by a number of authors to various stratified media problems. By definition,<sup>11</sup>

$$R_E ( ) = \frac{N_0 - Y_g}{N_0 + Y_g} .$$

$N_0$  is denoted (by transmission line analogy) as the self admittance of region 0 and  $Y_g$  is the surface admittance of the ground. Both  $N_0$  and  $Y_0$  depend upon the Sommerfeld integration variable  $\lambda$  as indicated below.

Specifically,

$$N_0 = \frac{Y_0}{j\omega\mu_0}$$

where  $\gamma_0 = \sqrt{\lambda^2 - k_0^2}$  and  $k_0^2 = \omega^2 \mu_0 \epsilon_0$ . The quantity  $Y_0 = Y_1$  is the admittance seen looking into layer 1 from layer 0. This admittance (from transmission line analogies<sup>10</sup>) can be shown to depend upon the self admittance  $N_m$  of each layer of thickness  $d_m$ , and the parameter  $\gamma_m$ , where

$$\gamma_m = \sqrt{\lambda^2 - k_m^2},$$

$$k_m^2 = \omega^2 \mu_0 \epsilon_0 - j\omega \mu_0 \sigma_m,$$

and

$$N_m = \frac{Y_m}{j\omega \mu_0}.$$

The "transmission line" equation which determines the interrelation between  $N_m$ ,  $\gamma_m$ , and  $d_m$ , and the admittance  $Y_m$  as seen looking from layer  $m-1$  into the layer  $m$  is

$$Y_m = N_m \frac{Y_{m+1} + 1 + N_m \tanh \gamma_m d_m}{N_m + Y_{m+1} \tanh \gamma_m d_m}$$

One determines  $Y_1 = Y_g$  as follows: Use the above "transmission line" equation starting at the  $N$ th layer and iterate up to the boundary between layers 0 and 1, assuming initially  $Y_N = N_N$ .

Also by definition,

$$R_M(\lambda) = \frac{K_0 - Z_g}{K_0 + Z_g},$$

where  $K_0$  is denoted as the self-impedance of free space and  $Z_g = Z_1$  is the surface impedance of the ground. The quantity  $Z_g$  is determined by using the "transmission line" equation

$$Z_m = K_m \frac{Z_{m+1} + 1 + K_m \tanh \gamma_m d_m}{K_m + Z_{m+1} \tanh \gamma_m d_m},$$

where

$$K_m = \frac{\gamma_m}{\sigma_m + j\omega\epsilon_m}.$$

One determines  $Z_1$  by an iterative procedure like that used for determining  $Y_1$ .

## NUMERICAL RESULTS

### HOMOGENEOUS MEDIA

The results presented in this section have been determined through use of the formulas discussed in the previous section. Calculations have been made for the following physical situations: In all cases, the height of the center of both the transmitting and receiving loops is 0.68 m above ground. Horizontal separation distances  $d$  between the transmitter and receiver loops of 5 and 10, have been considered. A frequency range of 0.1 to 21 MHz and relative dielectric constants

$\epsilon_r$  of 5, 10, and 25 were used in the calculation model. The conductivities considered and their associated alphanumeric designators, used in Figures 5 - 35, follow:

$\sigma = 10^{-4}$ (A),  $2 \times 10^{-4}$ (B),  $5 \times 10^{-4}$ (C),  $10^{-3}$ (D),  $2 \times 10^{-3}$ (E),  
 $5 \times 10^{-3}$ (F),  $10^{-2}$ (G),  $2 \times 10^{-2}$ (H),  $5 \times 10^{-2}$ (I),  $10^{-1}$ (J),  
 $2 \times 10^{-1}$ (K) mho/m.

Figures 6 - 11 illustrate the ratio of the magnitudes (in dB) and the difference of the phases for the coaxial/perpendicular case of the induced voltage in the receiving loop. The relative dielectric constant assumptions ( $\epsilon_r = 5, 10, 25$ ) and horizontal separation distances (5, 10m) are indicated in the figure captions. Figures 12-17 depict results for the coplanar/perpendicular case.

For those interested in using an absolute measurement technique, the mutual impedance for the coaxial, coplanar and perpendicular orientations for the various situations considered are presented in Figures 18-23 (coaxial), Figures 24-29 (coplanar), and Figures 30-35 (perpendicular).

By comparing Figures 6-8 which illustrate the coaxial/perpendicular results for a loop separation of 5 m, one can see the effect of the relative dielectric constant  $\epsilon_r$  upon the results.

Consequently, the larger  $\epsilon_r$  is the more frequency variation there is in the results. The lower frequency results ( $f \sim 0.1$  MHz) are essentially independent of  $\epsilon_r$ , whereas the higher frequency results ( $f \sim 20$  MHz) are quite different for the various cases of  $\epsilon_r$ .

This is as would be expected for  $f \sim 0.1$  MHz, since conduction currents ( $\sim \sigma$ ) dominate displacement currents ( $\sim \omega \epsilon_0 \epsilon_r$ ). The converse situation applies for  $f \sim 20$  MHz. Thus, the higher frequency results are quite useful in determining the relative dielectric constant of the ground. It is expected that the ground should have an  $\epsilon_r$  between 5 and 25 for frequencies of 0.1 - 21 MHz.

As a general rule, the lower the frequency, the better one is able to resolve the conductivity. This is due to the dominant influence at these frequencies of conduction currents ( $\propto \sigma$ ) relative to the influence of displacement currents ( $\propto \omega \epsilon_0 \epsilon_r$ ), as mentioned above.

Plots have been made with phases varying between either  $-180$  to  $+180$  deg or  $0$  to  $360$  deg. Some phase plots have almost vertical lines, i.e., the phases vary through almost a full  $360$  deg (e.g., see Figure 16 between 15 and 19 MHz). The phase results have all been computed modulo  $2\pi$ , and thus one can either add or subtract multiples of  $360$  deg to the indicated phase points. This means that one can displace the B, C, and D curves in Figure 16 at 17 MHz down to approximately  $-185$ ,  $-230$  and  $-240$  deg respectively, rather than considering them to be at their approximate phases of  $+175$ ,  $+130$  and  $+120$  deg respectively, as shown. Modulo  $2\pi$  differences in the other phase plots can be corrected accordingly.

By comparing the results in Figures 9-11 for  $d = 10m$  with the corresponding results in Figures 6-8 for  $d = 5m$ , it is noted that the larger the separation distance  $d$  is for a fixed  $\epsilon_r$ , the greater the variation in the results. This remark also holds for a comparison of the results in Figures 12-14 with the corresponding results in Figures 15-17.

In comparing the absolute results for the coaxial (Figures 18-23), coplanar (Figures 24-29) and perpendicular (Figures 30-35) orientations, it is seen that the perpendicular case is much more sensitive to the presence of the ground than either the coplanar or coaxial cases. This is as one would intuitively expect in that in the absence of the ground (free space) there is coupling for the coplanar and coaxial cases, but there is no coupling for the perpendicular case. Hence, the perpendicular case should indicate ground perturbations much more than the coplanar and coaxial cases.

#### STRATIFIED MEDIA

It is possible to consider such a wide variety of cases using the stratified media model that one quickly has to define those cases which he may likely encounter experimentally. Several models have been chosen for numerical computation. Hopefully, the cases which one might face experimentally will be similar to the computation models. If experimental results are not similar to either the homogeneous model results or the stratified media results presented herein, one can compute the loop performance using any

knowledge of or suspicion of a stratification profile. It then becomes a trial-and-error procedure to match experimental stratified media results with theoretical stratified media results. It should, however, be kept in mind that many experimental sites cannot be adequately represented by either a homogeneous ground or a vertically stratified ground. Hence one should make judicious use of all available site information in selecting sites suitable for two-loop ground conductivity measurements.

A sample illustration of coplanar/perpendicular results one would obtain for a homogeneous ground is shown in Figure 36 for a ground with a relative dielectric constant  $\epsilon_r = 9$  and various ground conductivities  $\sigma$ . The conductivities considered and their associated alphanumeric designators used in Figure 36 follow:

$\sigma = 10^{-4}$ (A),  $2 \times 10^{-4}$ (B),  $5 \times 10^{-4}$ (C),  $10^{-3}$ (D),  $2 \times 10^{-3}$ (E),  $5 \times 10^{-3}$ (F),  $10^{-2}$ (G),  $2 \times 10^{-2}$ (H),  $5 \times 10^{-2}$ (I),  $10^{-1}$ (J),  $2 \times 10^{-1}$  (K) mho/m. The ratios (in dB) and the differences of the phases for the coplanar/perpendicular case of the induced voltage in the receiving loop are considered. A separation of  $d = 5\text{m}$  is assumed.

In many experimental situations, a homogeneous layer of material may be covered by a second layer of another homogeneous material. A common example of this situation is depicted in Figure 37a. A moderately conducting overburden represented by  $\epsilon_r = 9$  and  $\sigma = 10^{-2}$  mho/m of thickness  $D_1 = 0.5$  m lays over a second medium with  $\epsilon_r = 9$  and  $\sigma$ 's between  $10^{-4}$  and  $2 \times 10^{-1}$  mho/m. For lower layer conductivities

of the order of  $10^{-7}$  mho/m, the two-loop technique would indicate an effective ground conductivity  $10^{-2}$  mho/m and  $10^{-1}$  mho/m. For lower layer conductivities of the order of  $10^{-1}$  mho/m, the two-loop technique would indicate an effective ground conductivity  $> 10^{-2}$  mho/m and  $< 10^{-1}$  mho/m. These statements are illustrated by a comparison of the respective homogeneous ground results shown in Figure 36 with appropriate layered ground results shown in Figure 38, where the same alphanumeric designators are used. It is quite evident from this comparison that a small layer of moderately conducting overburden can effectively mask the presence of a low-conductivity subsurface. This is as would be intuitively expected.

A major question of interest is: How significant an influence does the thickness of the overburden have upon the two-loop response? This is perhaps best illustrated by means of the two-loop responses for a variety of situations such as those depicted in Figures 37b, c, d, and e. Figures 39 through 43 depict such results. In these figures, the thicknesses  $D$  of the upper layer considered and their alphanumeric designators are: 0.1(A), 0.5(B), 1.0(C), 5.0(D), 10.0(E), 50.0(F), m. A comparison of each of these situations with the homogeneous ground results shown in Figure 36 lead to the following conclusions:

1. From Figure 39, which depicts the use shown in Figure 37b, it is noted that the thicker overburden, the more the overburden dominates the measurement, giving a  $\sigma = 10^{-4}$  for the "A" curve ( $D = 0.1$  m) and a  $\sigma = 10^{-2}$  for its "F" curve ( $D = 50$  m).

2. In Figure 40 for the Figure 37c case, the reverse situation is seen. This is due to the interchange of the high-conductivity and low-conductivity layers. Thus in this case the thicker the upper layer, the more nearly the conductivity matches the value for that layer and the smaller the influence of the higher conducting subsurface layer.

3. Figures 37d and e are analogous to Figures 37b and c, except that the higher conductivity value is  $10^{-3}$  mho/m. The corresponding numerical results are illustrated in Figures 41 and 42. The results show the same trends as for the corresponding situations in Figures 39 and 40, respectively, except that the results are not as dramatic due to the closer match of upper and lower layer conductivities.

Another ground condition which might be encountered is depicted in Figure 37f. A higher conducting layer is sandwiched between two low-conductivity layers. Such a situation might be encountered, for example, in a permafrost region with a permanently frozen lower layer, an upper layer which is frozen, and a middle layer which is not frozen. This might result in the conductivities as indicated. Various combinations of  $D_1$  and  $D_2$  were considered.

The results are shown in Figure 43 where the sum  $D_1 + D_2 = 0.5$  m and the alphanumeric indicators associated with  $D_2$  are: 0.05(A), 0.1(B), 0.3(C), and 0.5(D),m. The significant effect of the higher conductivity layer upon the two-loop response is quite evident for the lower frequencies. That is, as the thickness  $D_2$  increases, the low-conductivity subsurface is more effectively masked by the higher conductivity middle layer.

#### VALIDITY OF APPROXIMATE FORMULAE

Some interest exists in the range of validity of various appropriate techniques used to determine the coupling between two loops operated in the near presence of the ground. Two approximate procedures were tried by the authors in an attempt to determine simple formulas describing the loop dependence upon  $h$  and  $d$ . These approximate results were then compared with numerical evaluations of the exact Sommerfeld integrals. This was the test used to check the validity of the approximate procedures.

The two approximations tried were the usual quasistatic approximation<sup>1,2-5,8</sup> of  $k_{\text{air}} - 0$  (or assuming all dimensions are small compared to a free space wavelength) and the approximation of the reflection coefficients  $R_E(\lambda)$  and  $R_M(\lambda)$  in the Sommerfeld integrals by their plane wave counterparts.<sup>13</sup> The reflection coefficient approximation yielded little to no agreement with the exact results and was abandoned as a suitable approximation for the parameters considered.

The quasistatic approximation was quite well matched to the exact results for frequencies such that  $h < d \lambda/10$ , or for the parameters considered,  $f < 6$  MHz for  $d = 5$  m and  $f < 3$  MHz for  $d = 10$  m. For frequencies greater than this quasistatic limit, the results were sometimes quite well matched--at least for the parameters considered. Examples illustrating typical results for  $\epsilon_r = 5$ ,  $h = 0.68$  m, and  $d = 5$  are shown in Figures 44 (coaxial/perpendicular case). For the situations presented in these figures, the quasistatic results are good to within 6 dB and  $30^\circ$  for  $f < 10$  MHz. For many situations the quasistatic and exact results have a high degree of correlation, even up to 21 MHz. Thus, no precise definition of the range of utility of the quasistatic approximation can be made, other than it is definitely valid and useful for  $d < \lambda/10$ .

#### ADDITIONAL COMMENTS

The method described herein provides a measurement of the effective-conductivity of the ground as observed at the surface. If the ground is stratified and has a surface layer with a high conductivity, this will dominate the measurement. Hence, the method is insensitive to deep, low-conductivity subsurfaces. For this reason it cannot be regarded as suitable for a determination of the conductivity of a low-conductivity soil layer when the latter is greater than about two-tenths of a skin depth thick.

For a site where the actual conductivity decreases with depth, the measured conductivities will characteristically increase with an increase in frequency. Conversely, a medium for which the conductivity

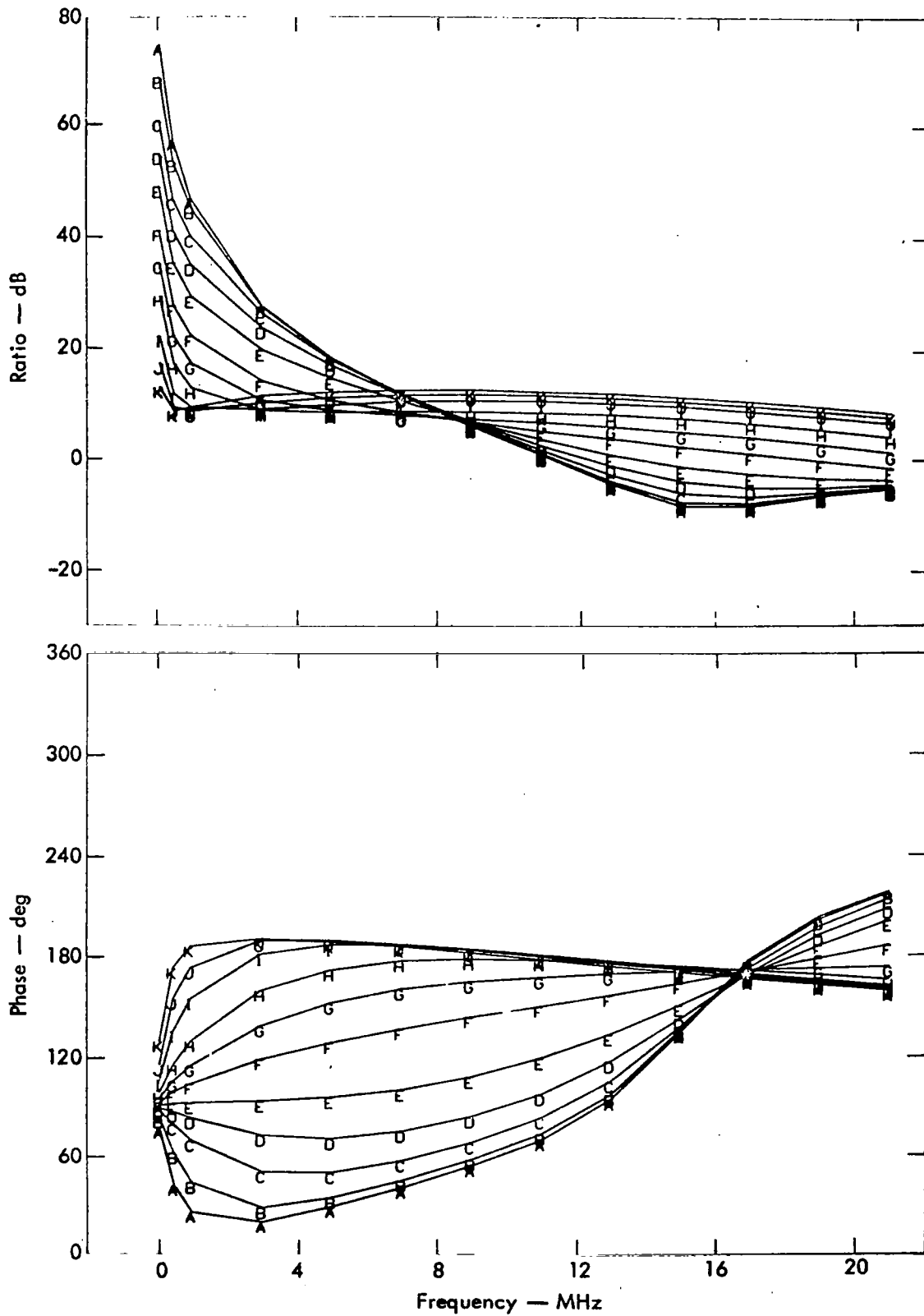


Fig. 6. Coaxial/perpendicular mutual impedance:  $\epsilon_r = 5$ ,  $d = 5$ .

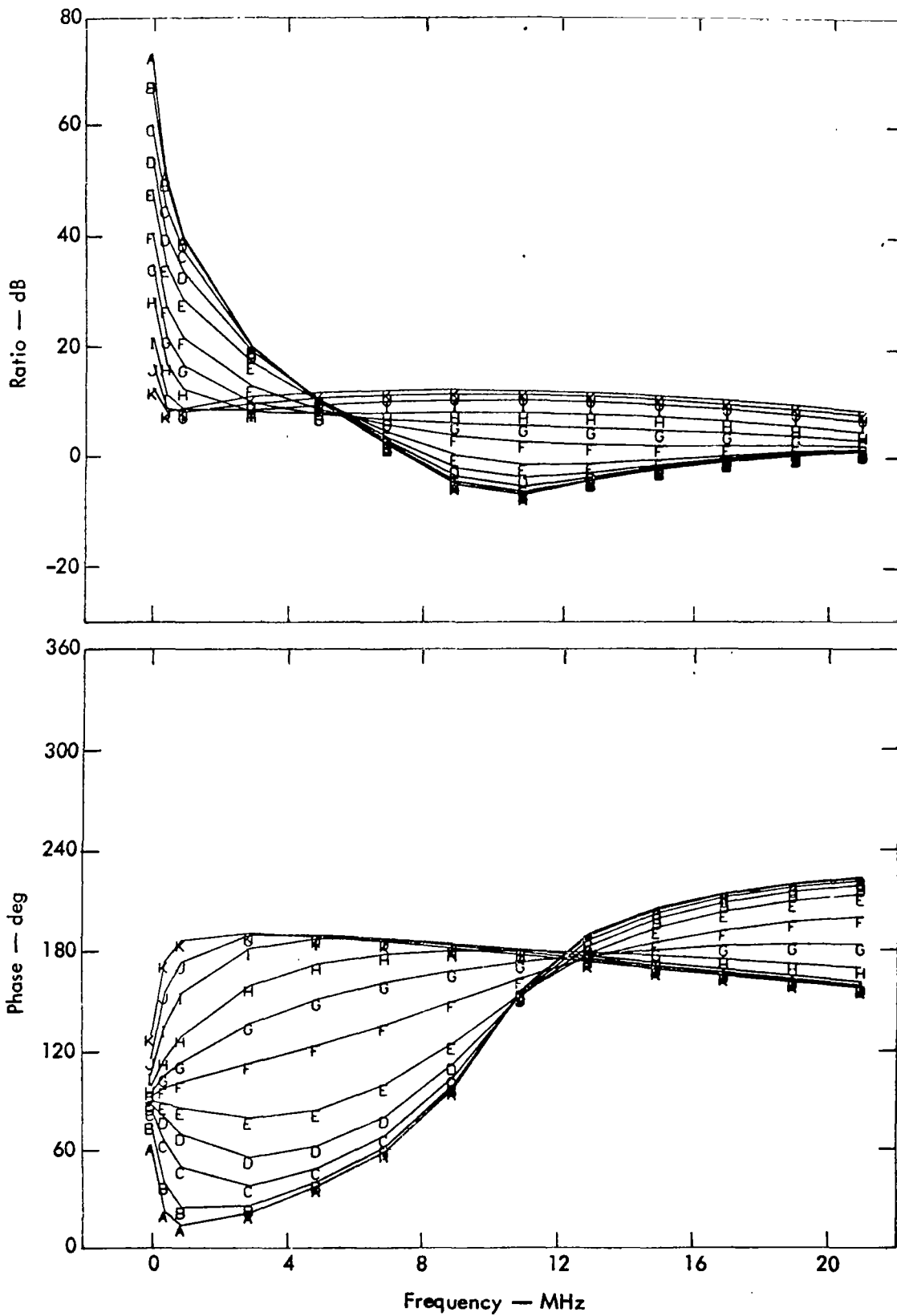


Fig. 7. Coaxial/perpendicular mutual impedance:  $\epsilon_r = 10$ ,  $d = 5$ .

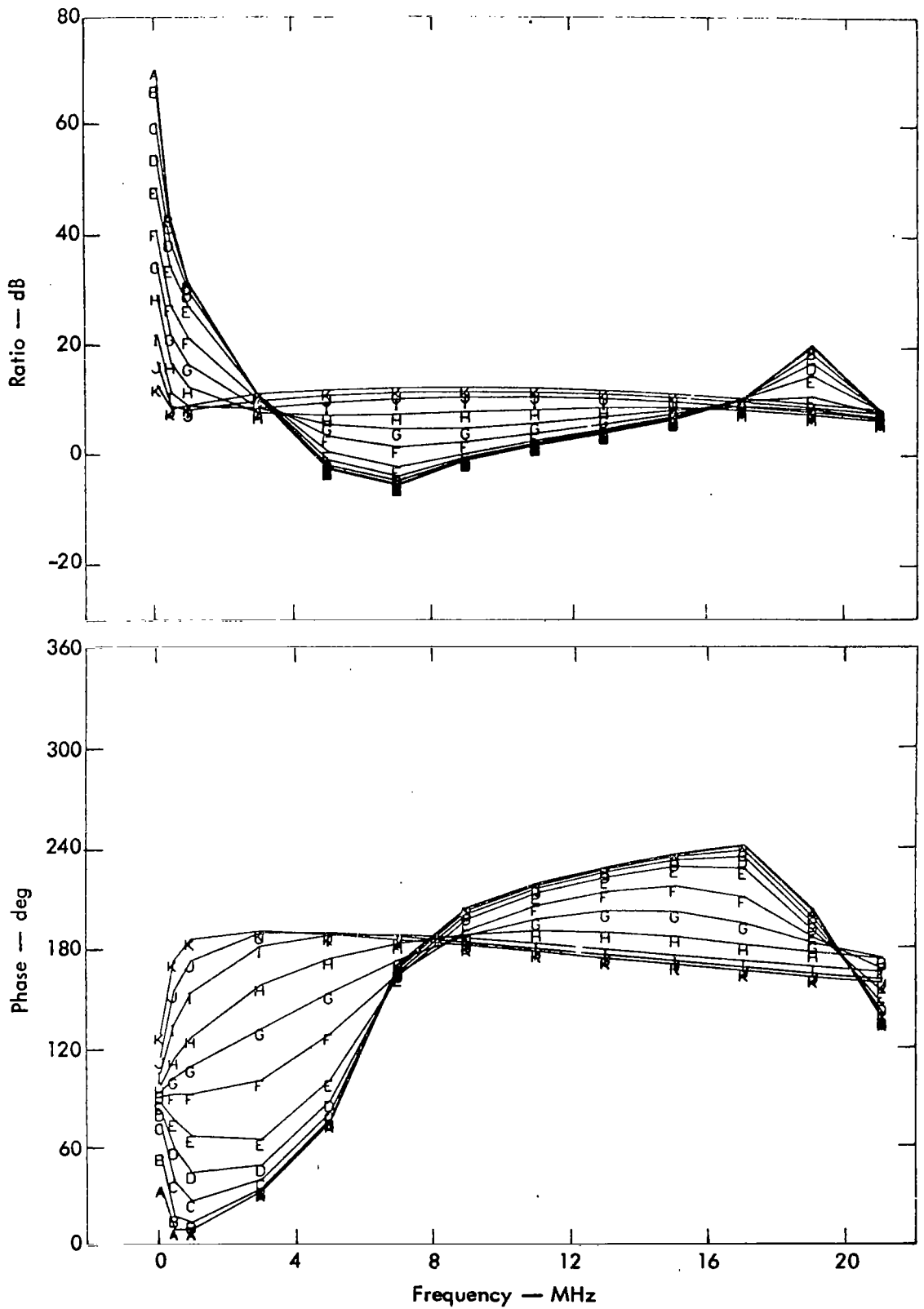


Fig. 8. Coaxial/perpendicular mutual impedance:  $\epsilon_r = 25$ ,  $d = 5$ .

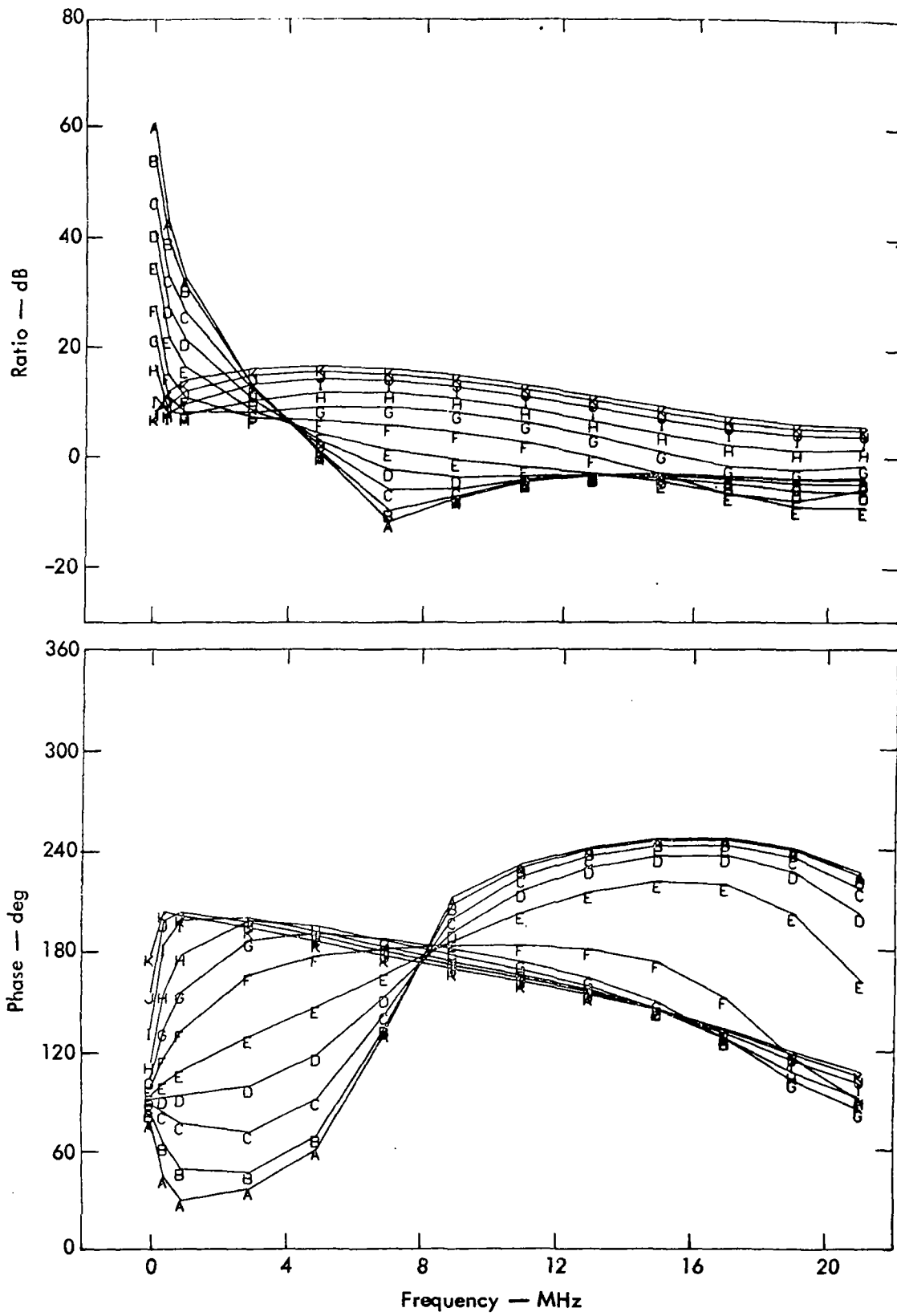


Fig. 9. Coaxial/perpendicular mutual impedance:  $\epsilon_r = 5$ ,  $d = 10$ .

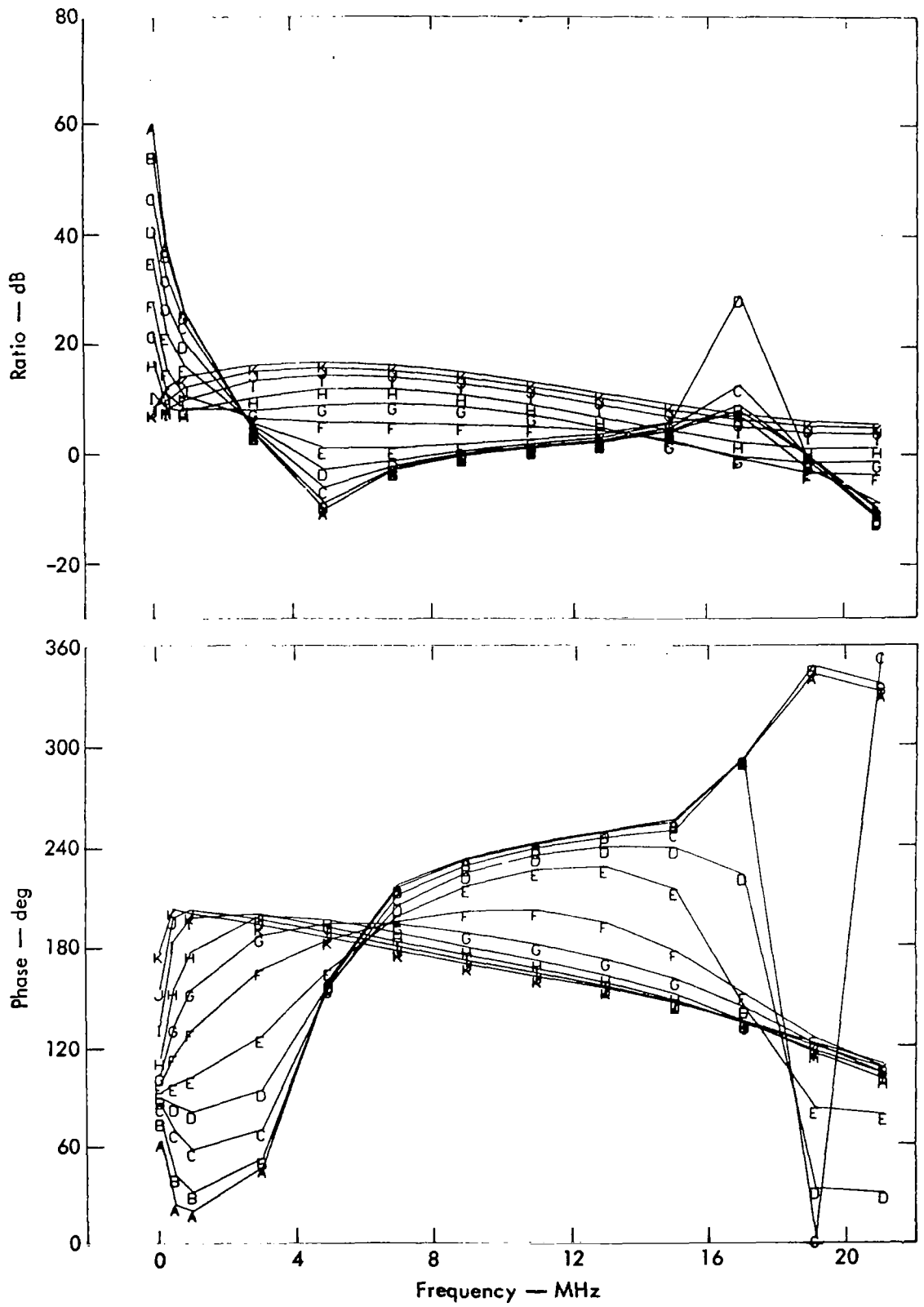


Fig. 10. Coaxial/perpendicular mutual impedance:  $\epsilon_r = 10$ ,  $d = 10$ .

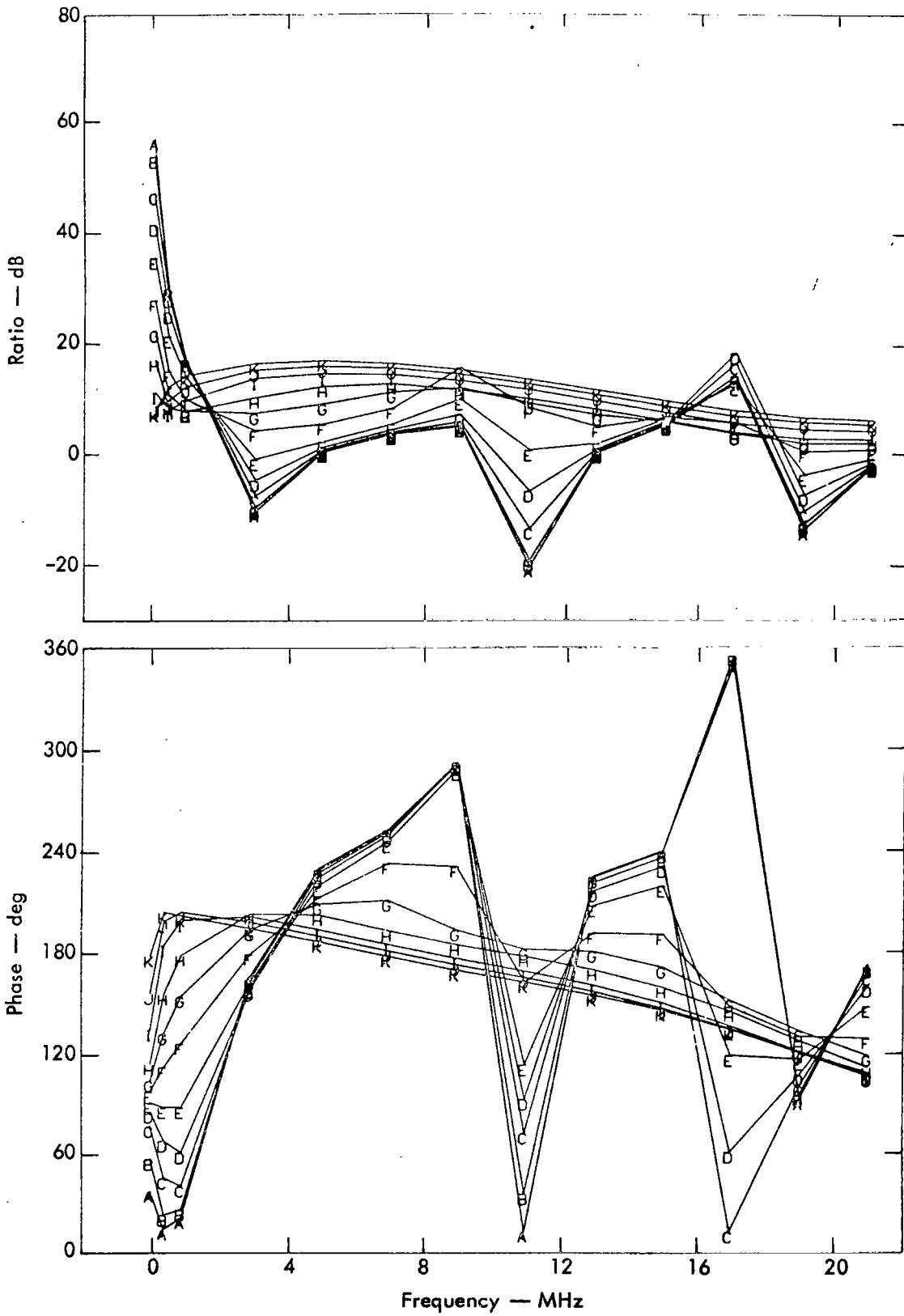


Fig. 11. Coaxial/perpendicular mutual impedance:  $\epsilon_r = 25$ ,  $d = 10$ .

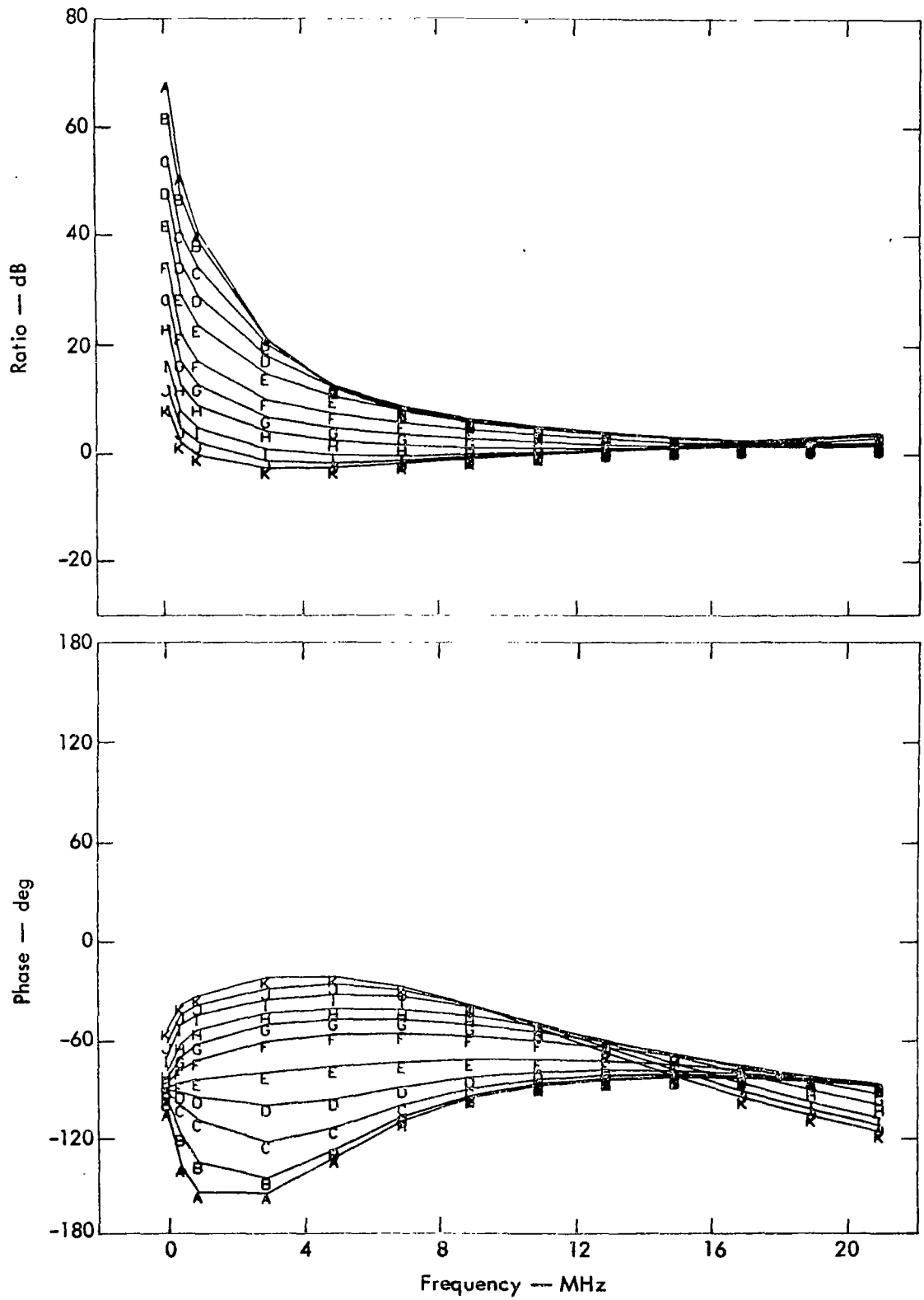


Fig. 12. Coplanar/perpendicular mutual impedance:  $\epsilon_r = 5$ ,  $d = 5$ .

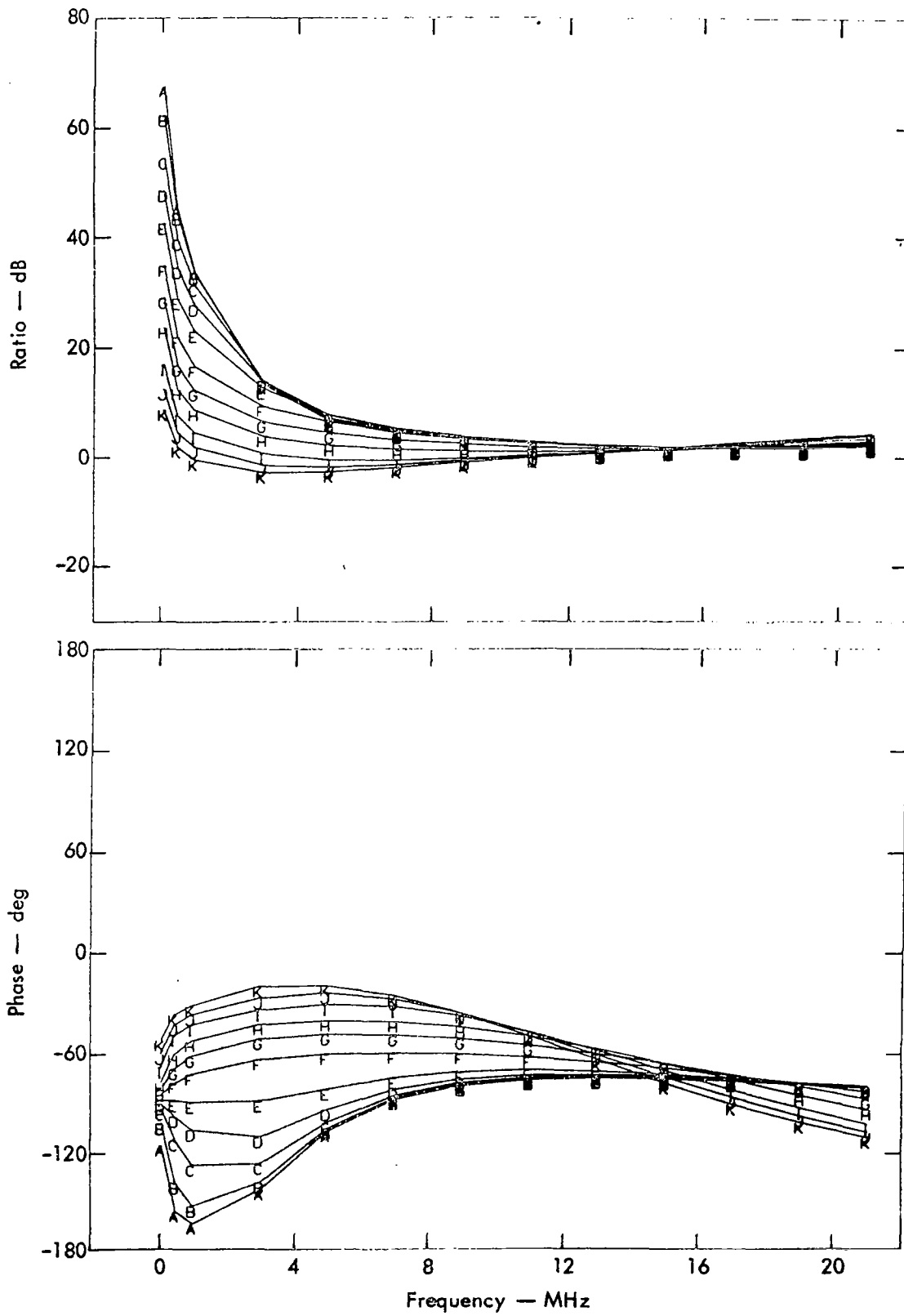


Fig. 13. Coplanar/perpendicular mutual impedance:  $\epsilon_r = 10$ ,  $d = 5$ .

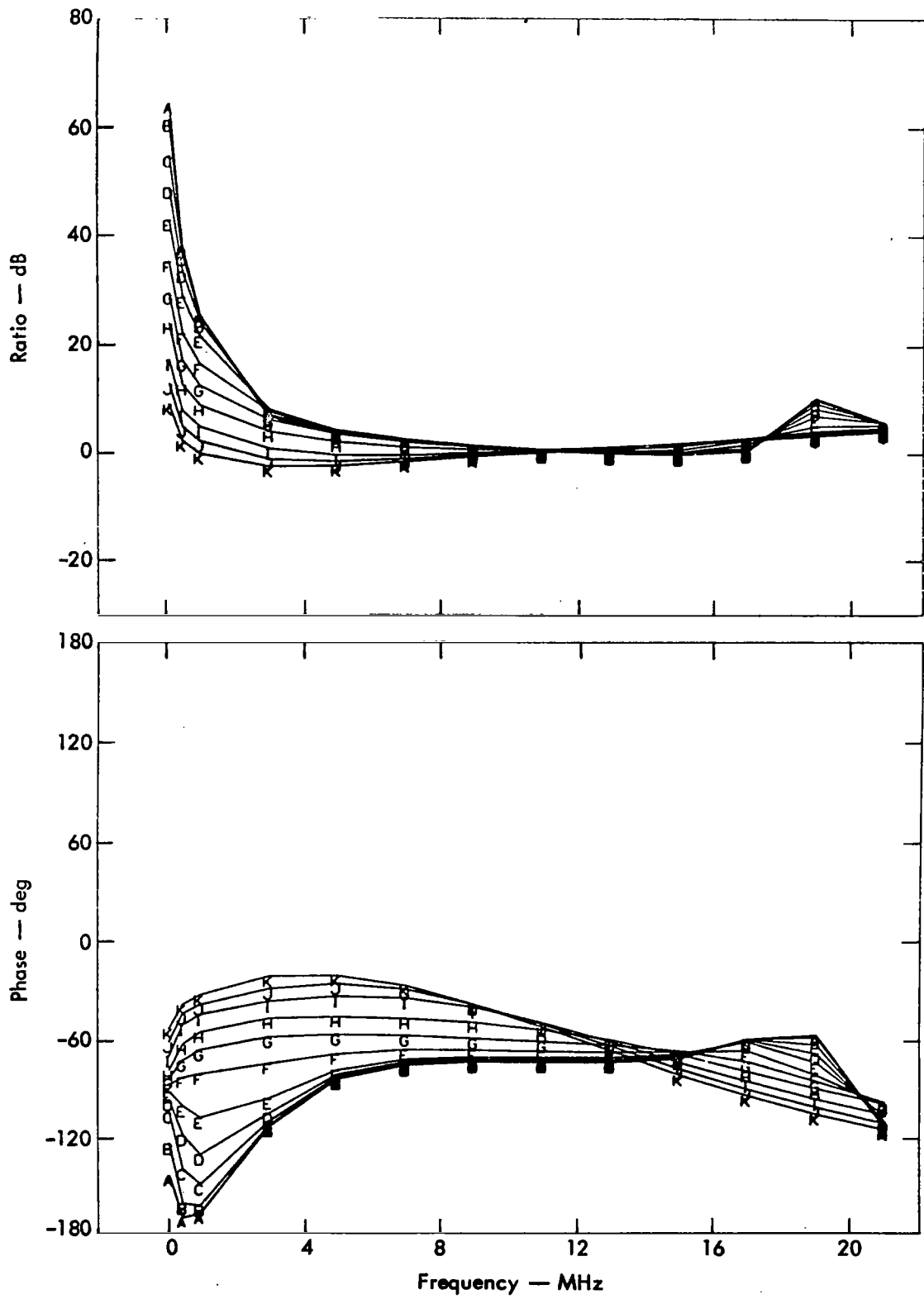


Fig. 14. Coplanar/perpendicular mutual impedance:  $\epsilon_r = 25$ ,  $d = 5$ .

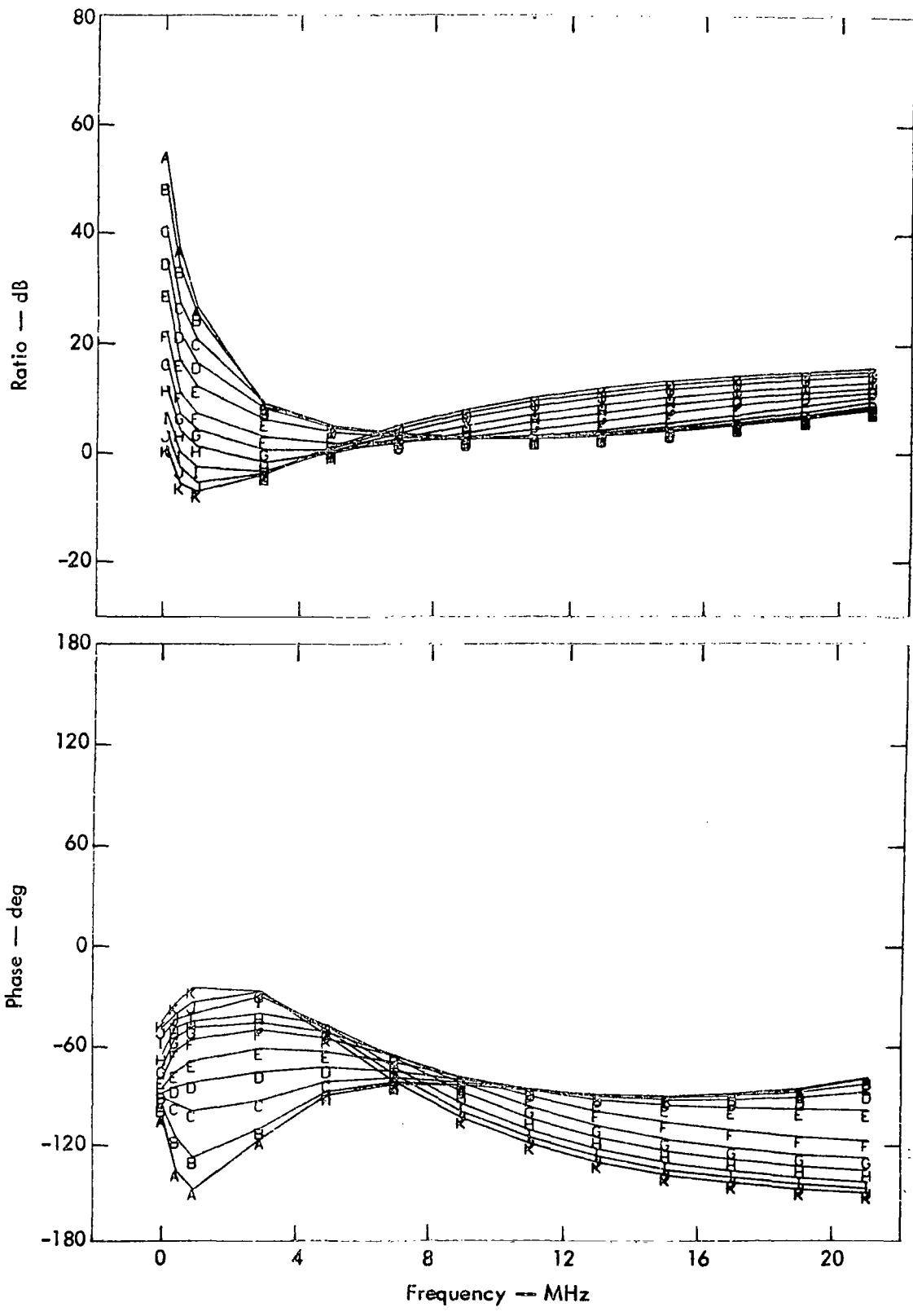


Fig. 15. Coplanar/perpendicular mutual impedance:  $\epsilon_r = 5$ ,  $d = 10$ .

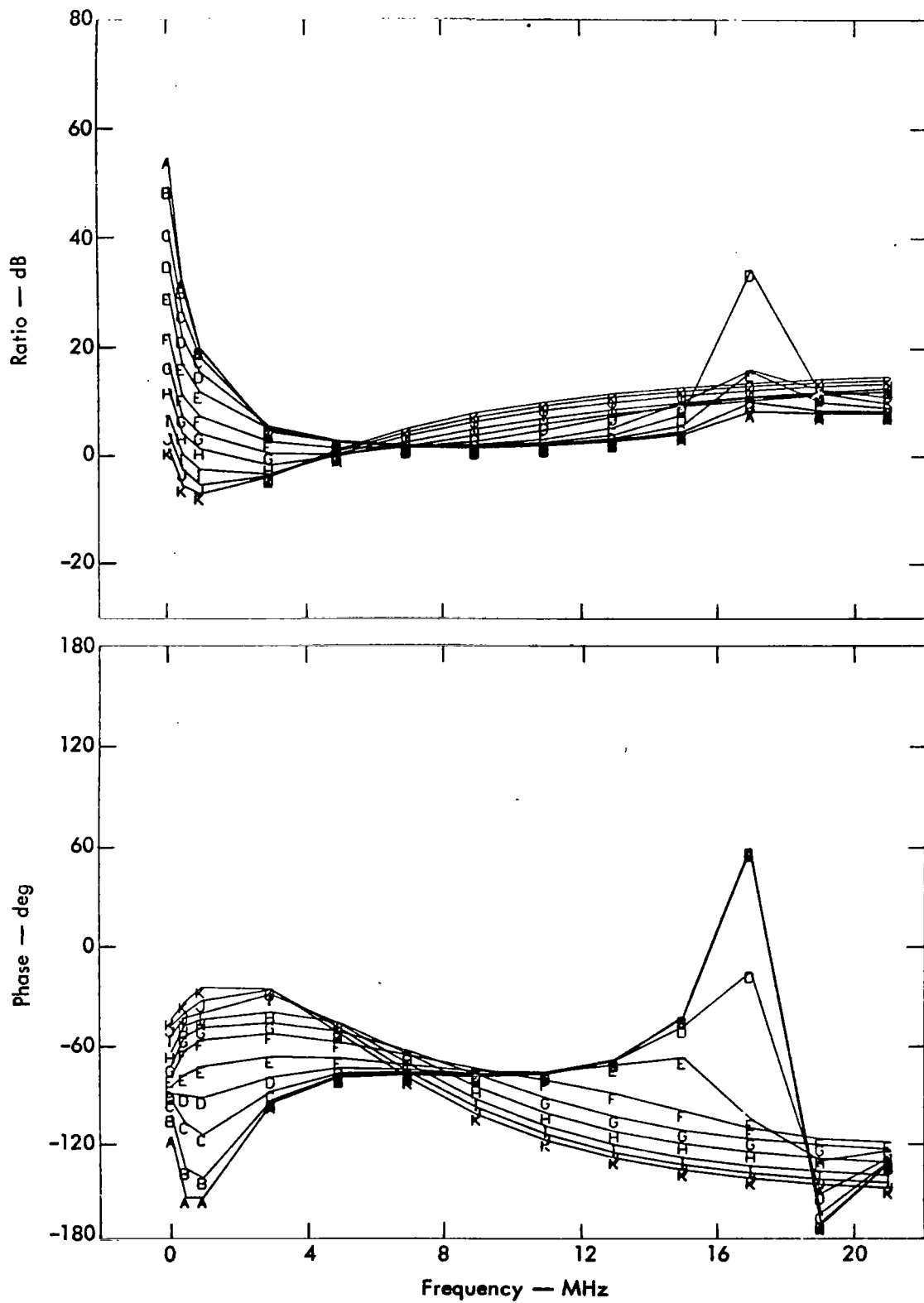


Fig. 16. Coplanar/perpendicular mutual impedance:  $\epsilon_r = 10$ ,  $d = 10$ .

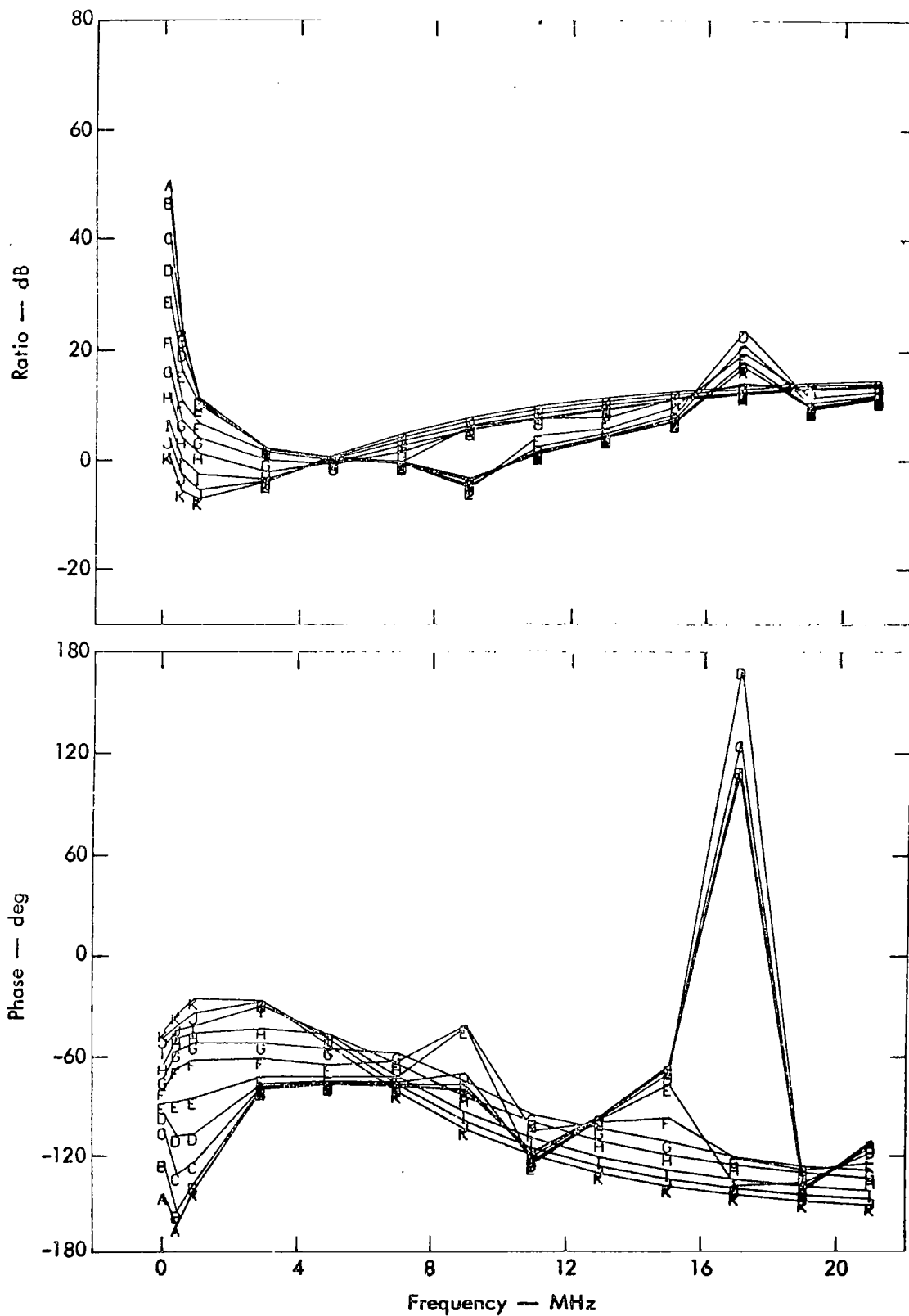


Fig. 17. Coplanar/perpendicular mutual impedance:  $\epsilon_r = 25$ ,  $d = 10$ .

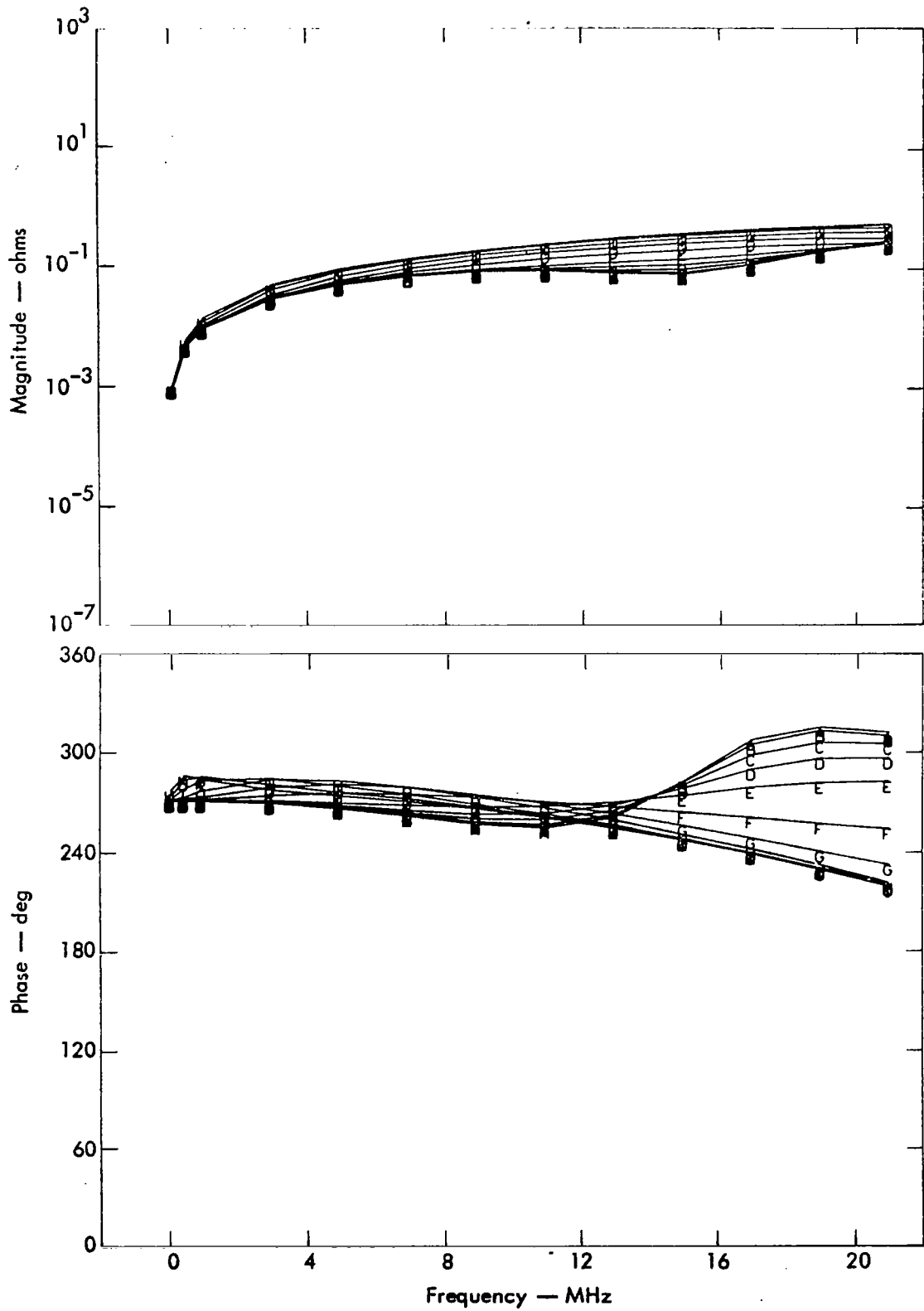


Fig. 18. Coaxial mutual impedance:  $\epsilon_r = 5$ ,  $d = 5$ .

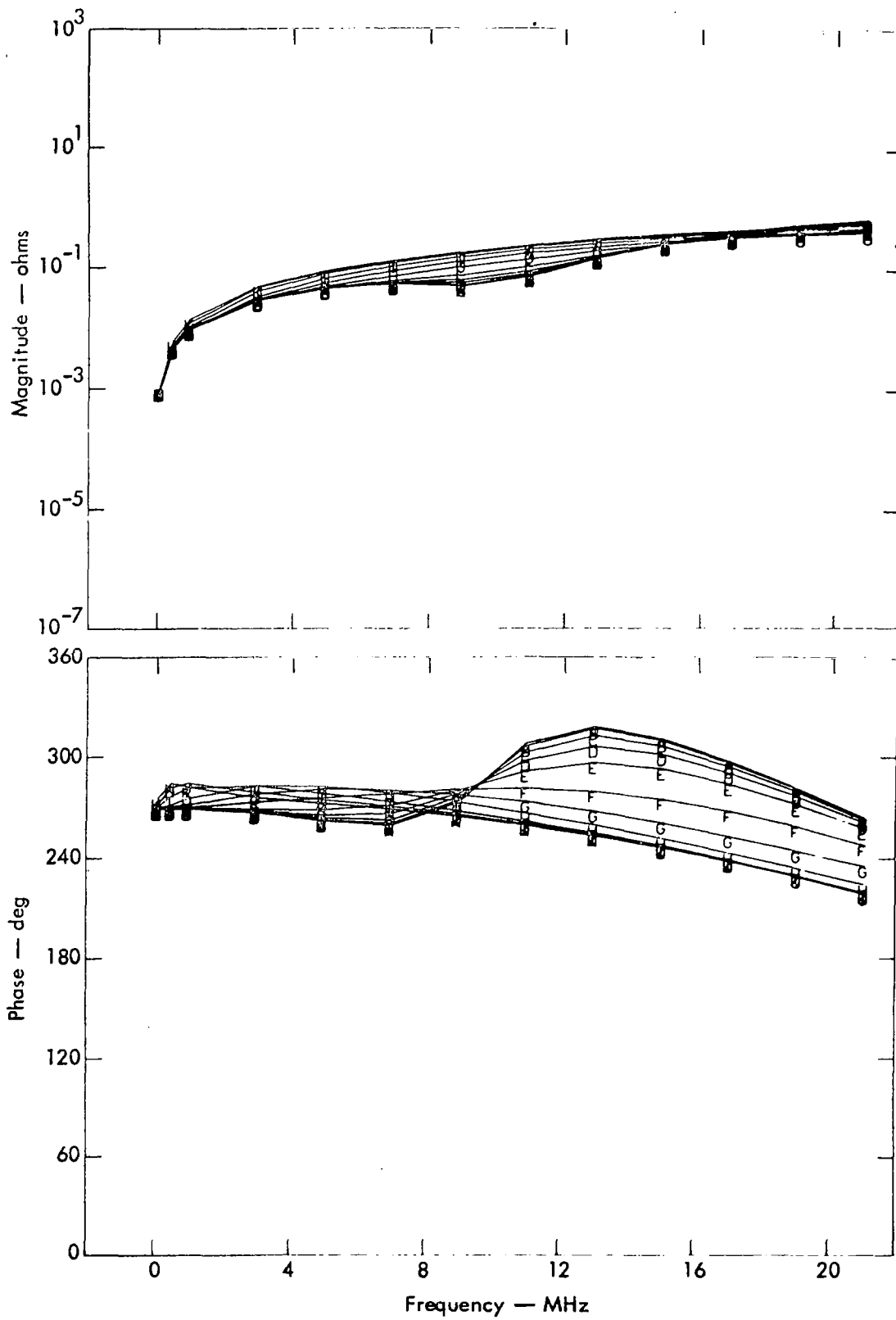


Fig. 19. Coaxial mutual impedance:  $\epsilon_r = 10$ ,  $d = 5$ .

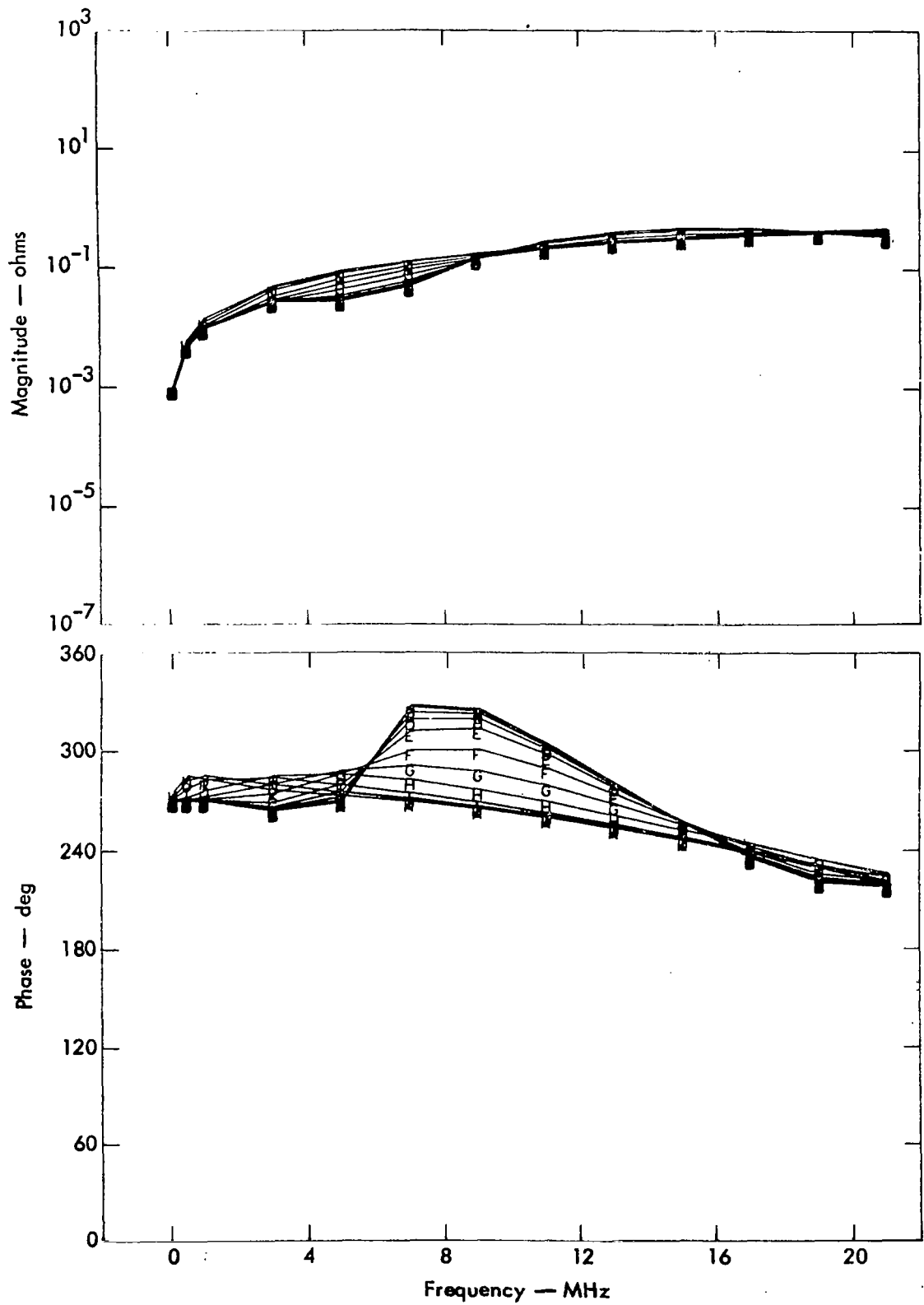


Fig. 20. Coaxial mutual impedance:  $\epsilon_r = 25$ ,  $d = 5$ .

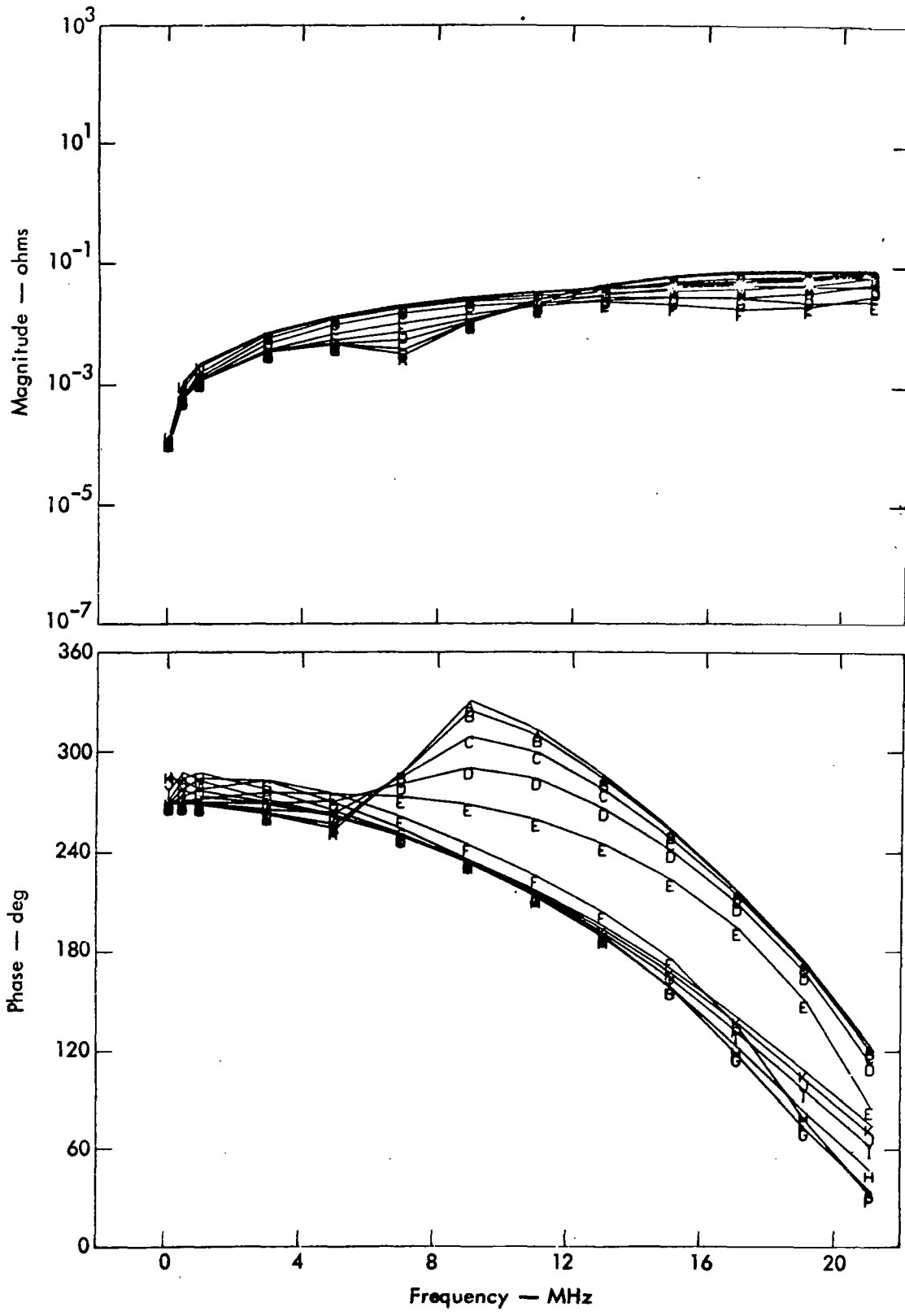


Fig. 21. Coaxial mutual impedance:  $\epsilon_r = 5$ ,  $d = 10$ .

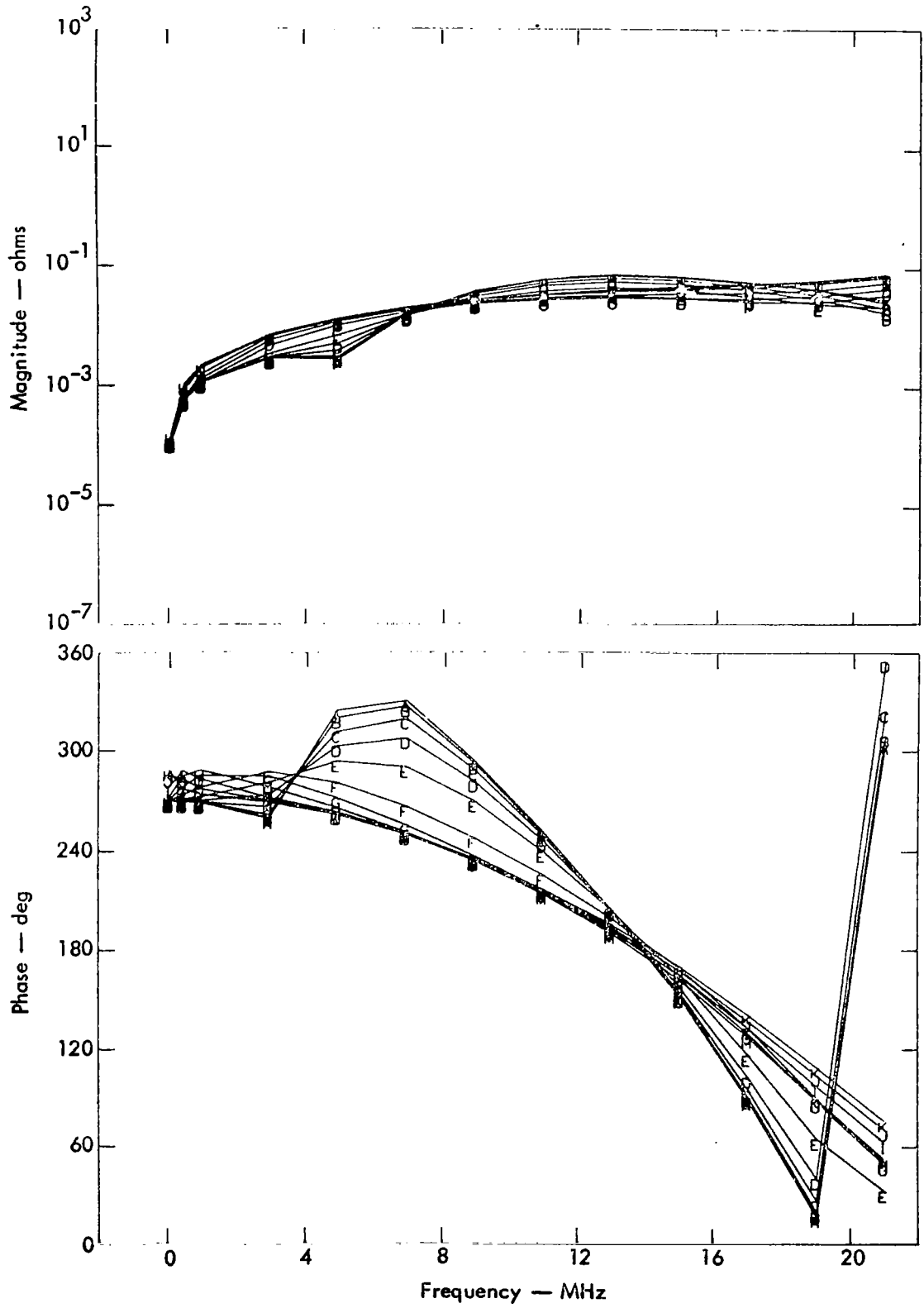


Fig. 22. Coaxial mutual impedance:  $\epsilon_r = 10$ ,  $d = 10$ .

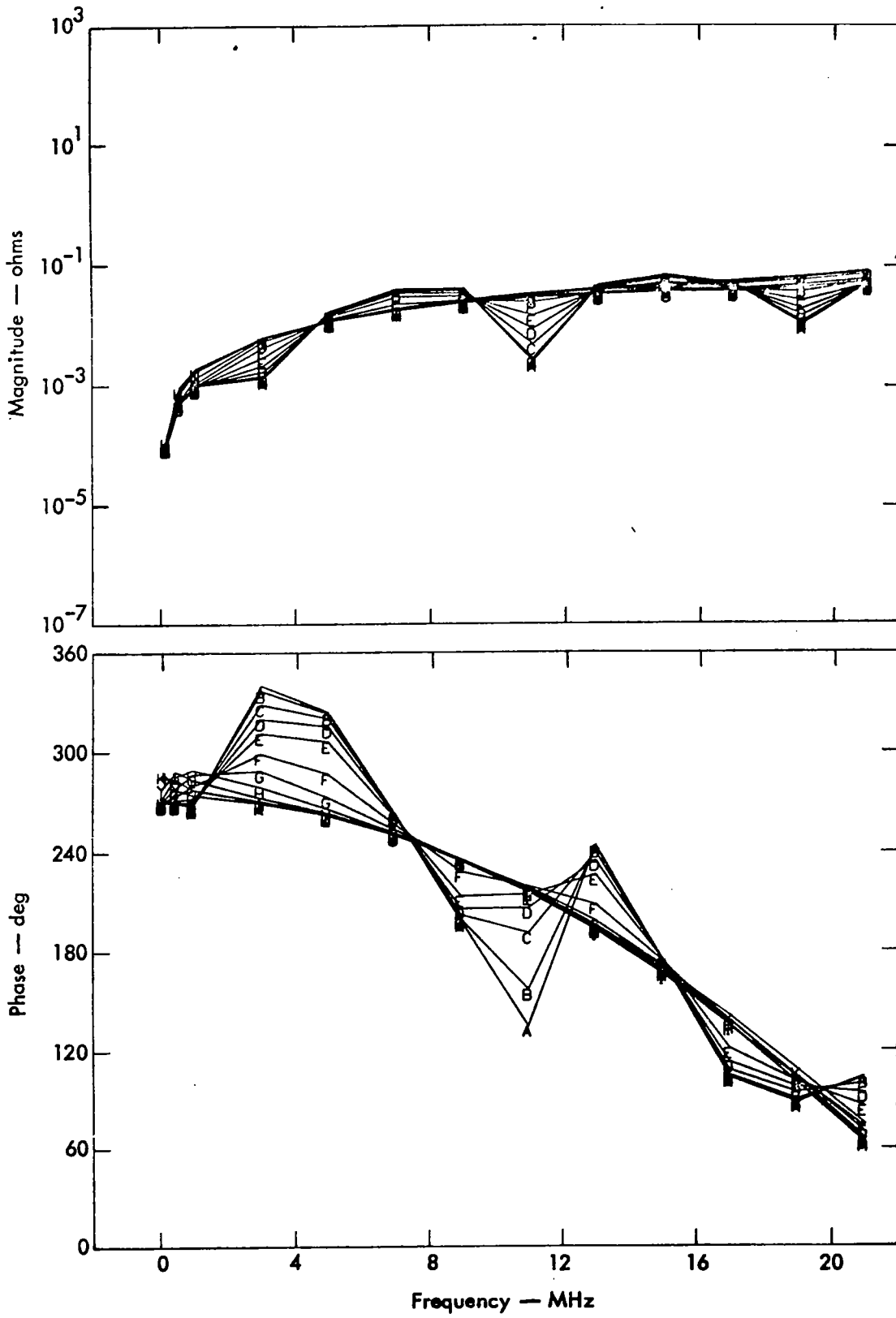


Fig. 23. Coaxial mutual impedance:  $\epsilon_r = 25$ ,  $d = 10$ .

increases with depth would be characterized by a measured conductivity which decreases as the frequency increases. These statements are founded upon the fact that lower frequencies typically penetrate more deeply into a conducting medium than do higher frequencies. Hence, the lower frequency results sample, or average, the results over a larger volume than do the higher frequencies.

A related and sometimes confusing result is that typically conductivity increases with frequency, and relative dielectric constant decreases with frequency. Determining what part of the frequency variation of in situ data is due to the subsurface structure and what part is due to the inherent frequency variation of the material is sometimes difficult. Fortunately, sometimes only the total effect is of interest. In situations where the earth is stratified, the specific computed results presented herein may not be applicable (i.e., an inexact model). If one encounters an unexpected and unusual experimental variation of induced voltage with frequency, he would be prudent to consider a variety of different subsurface strata thicknesses, conductivities, and relative dielectric constants which are physically reasonable to see if a model could be found that reproduces the experimental data. Unfortunately, the inverse problem of finding what is the medium from given field data is not as advanced a state of the art as the forward problem of calculating field data for a given medium. Much work is being done on the inverse problem and some rules of thumb <sup>12</sup> have resulted,

so the problem is not as hopeless as one might think. Additional information about the subsurface geology, topography, or local inhomogeneities aids significantly in providing such solutions.

It should be mentioned that the loop height ( $h = 0.68$  m) and the separation were arbitrarily chosen. That is, no detailed consideration has been made of the best height and separation for ease in determining  $\sigma$  and  $\epsilon_r$ . The distances used were chosen for the ease of the measurement and because these distances had been previously used in another system.<sup>6</sup>

#### CONCLUSIONS

1. The perpendicular orientation is the most sensitive to the presence of the ground.
2. The coplanar, coaxial, and perpendicular orientation cases are readily adapted for a generally stratified ground.
3. For a fixed separation distance  $d$ , the larger the  $\epsilon_r$  the more variation of the results with frequency.
4. For a fixed  $\epsilon_r$ , the larger separation of  $d = 10$  m has more variation of the results with frequency than the smaller separation of  $d = 5$  m.
5. The quasistatic approximation results and the exact Sommerfeld integral evaluations yield approximately the same results for  $f < 6$  MHz for  $d = 5$  m and  $h = 0.68$  m.
6. A ratio method is proposed because it eliminates any uncertainties based upon absolute measurements.

7. A swept-frequency method is proposed because it enables one to detect anomalies perhaps missed using selected cw frequencies. In addition, the relative time required and the ease of the experiment favors the sweep method over selected cw frequencies.

8. The method enables one to make in situ measurements and to monitor the results as a function of environmental conditions. This is an advantage in that small laboratory samples might yield results unrepresentative of the actual site.

9. The method is particularly well-suited for field evaluation tests of proposed antenna sites.

10. The use of a sweep method overcomes the practical detail of the need for a high-power, wide-band balun for use in a pulse-excited loop. A pulse system should be good for detecting ground anomalies, whereas a sweep system should be good for determining the ground constitutive parameters.

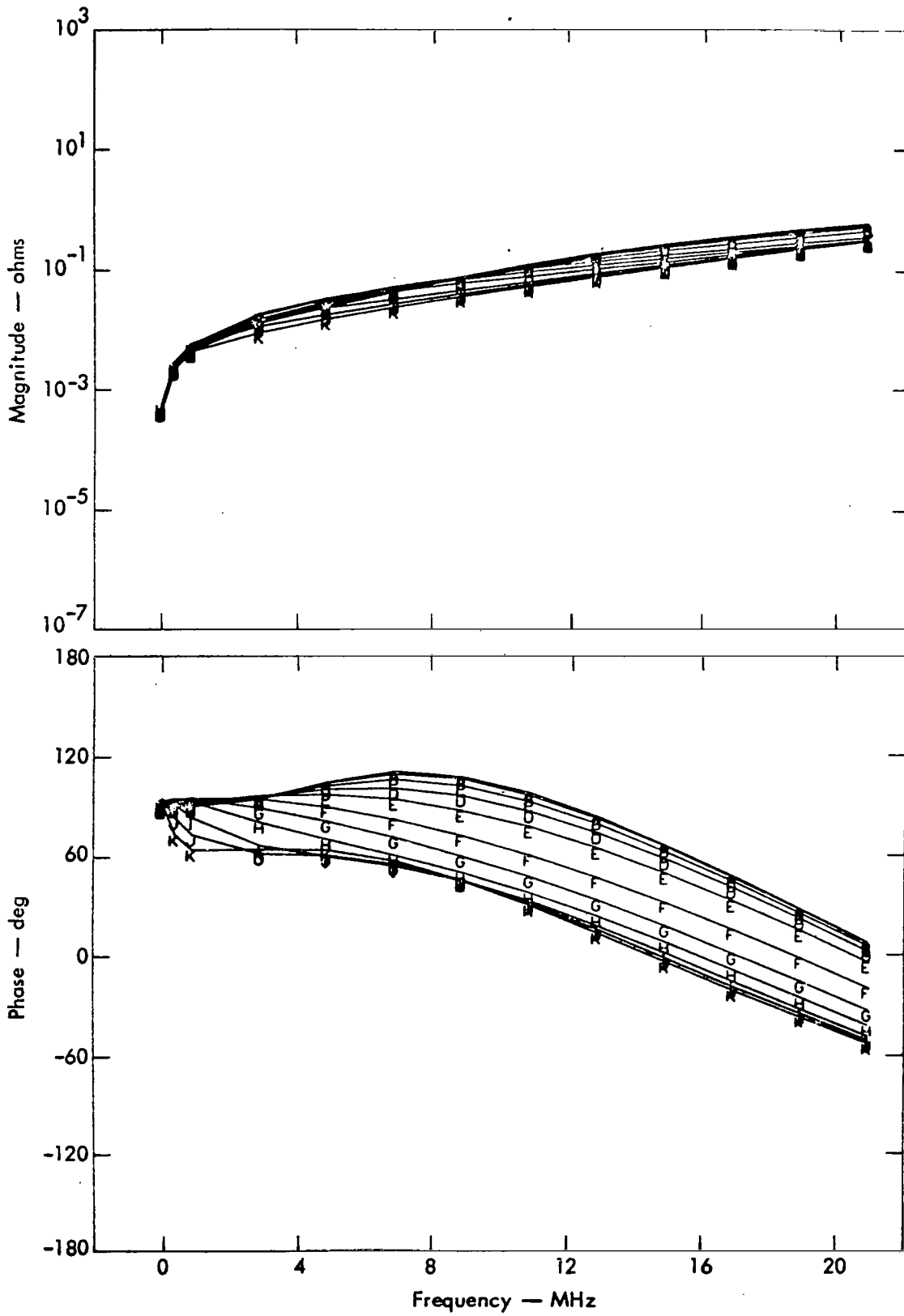


Fig. 24. Coplanar mutual impedance:  $\epsilon_r = 5$ ,  $d = 5$ .

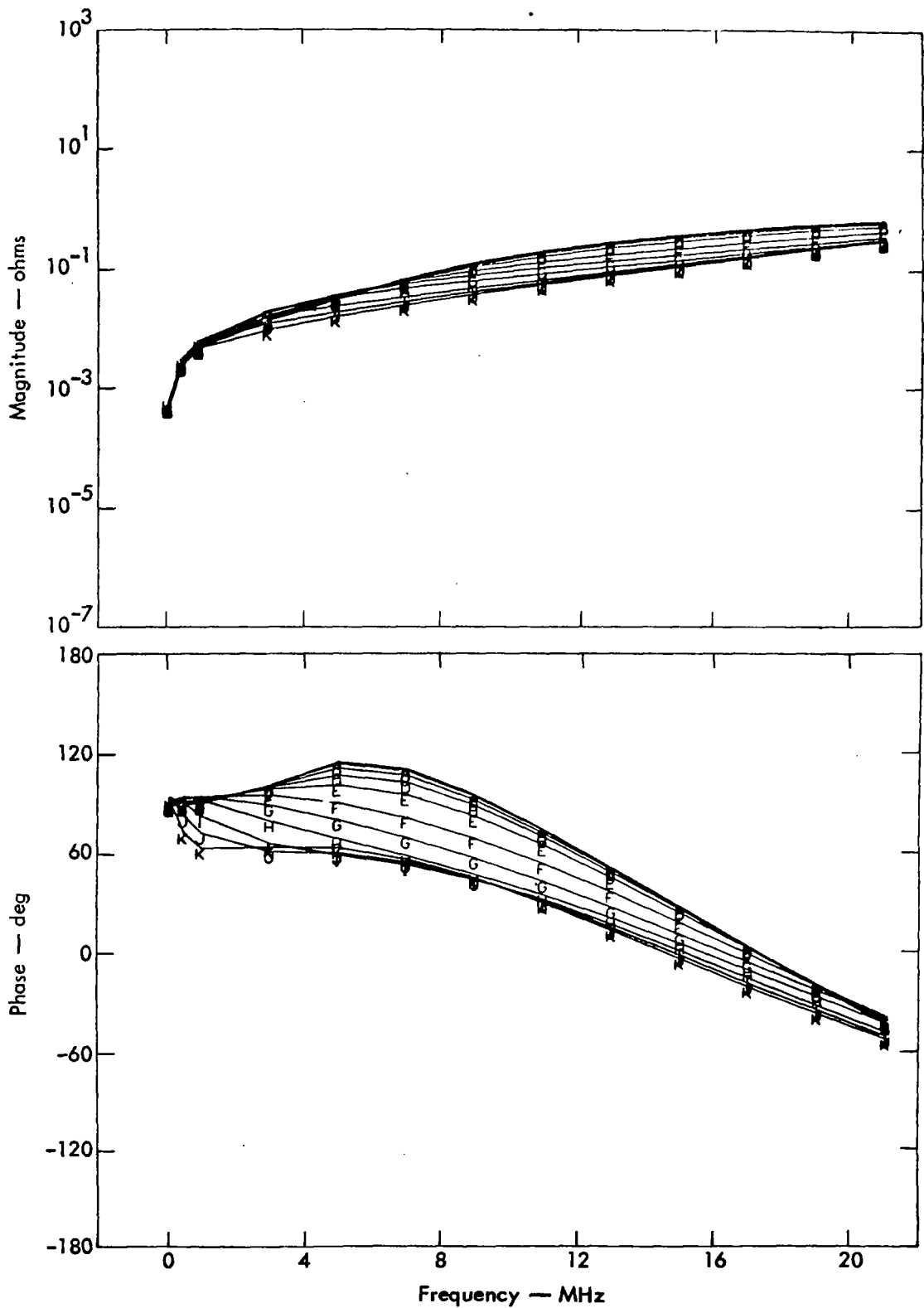


Fig. 25. Coplanar mutual impedance:  $\epsilon_r = 10$ ,  $d = 5$ .

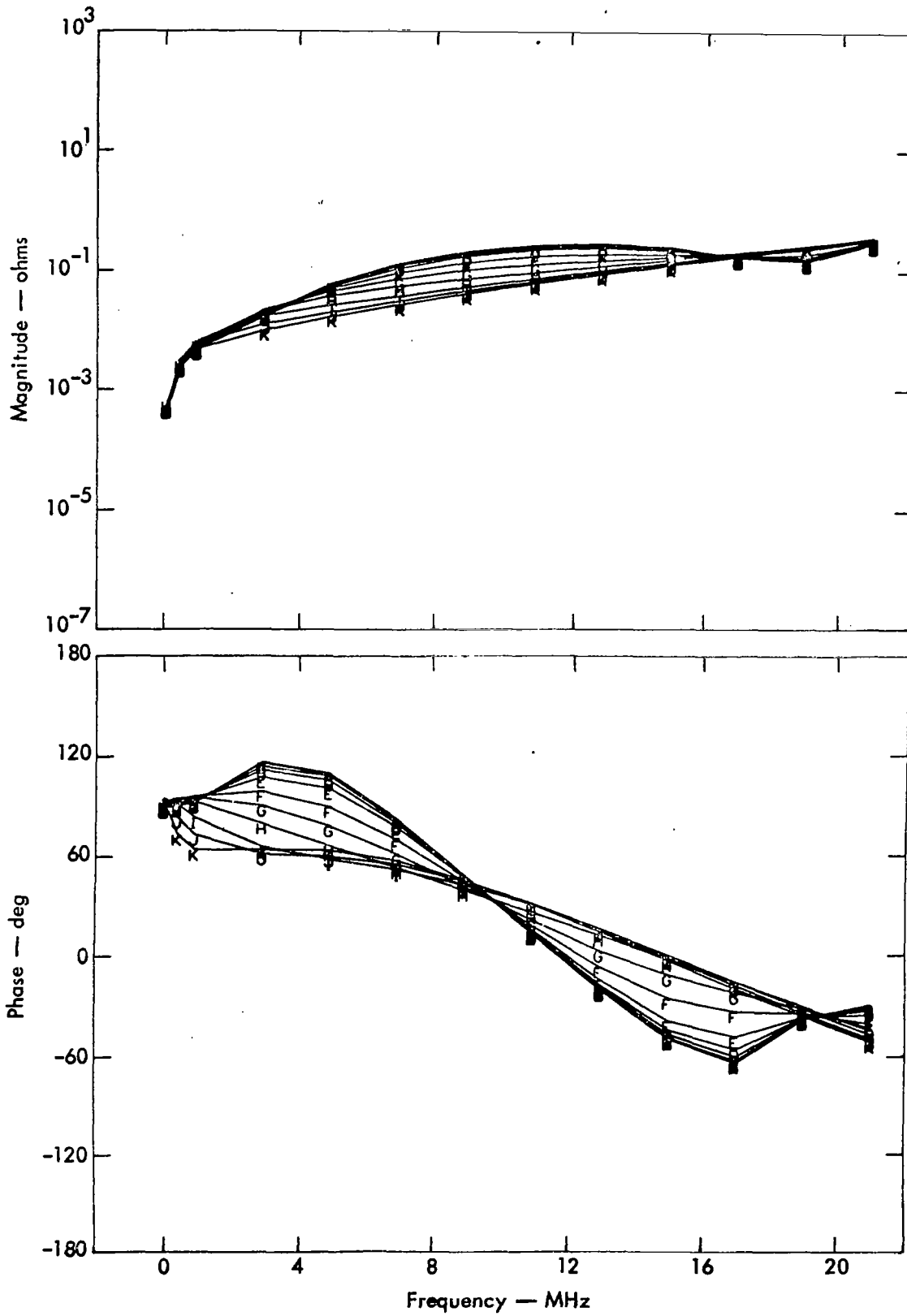


Fig. 26. Coplanar mutual impedance:  $\epsilon_r = 25$ ,  $d = 5$ .

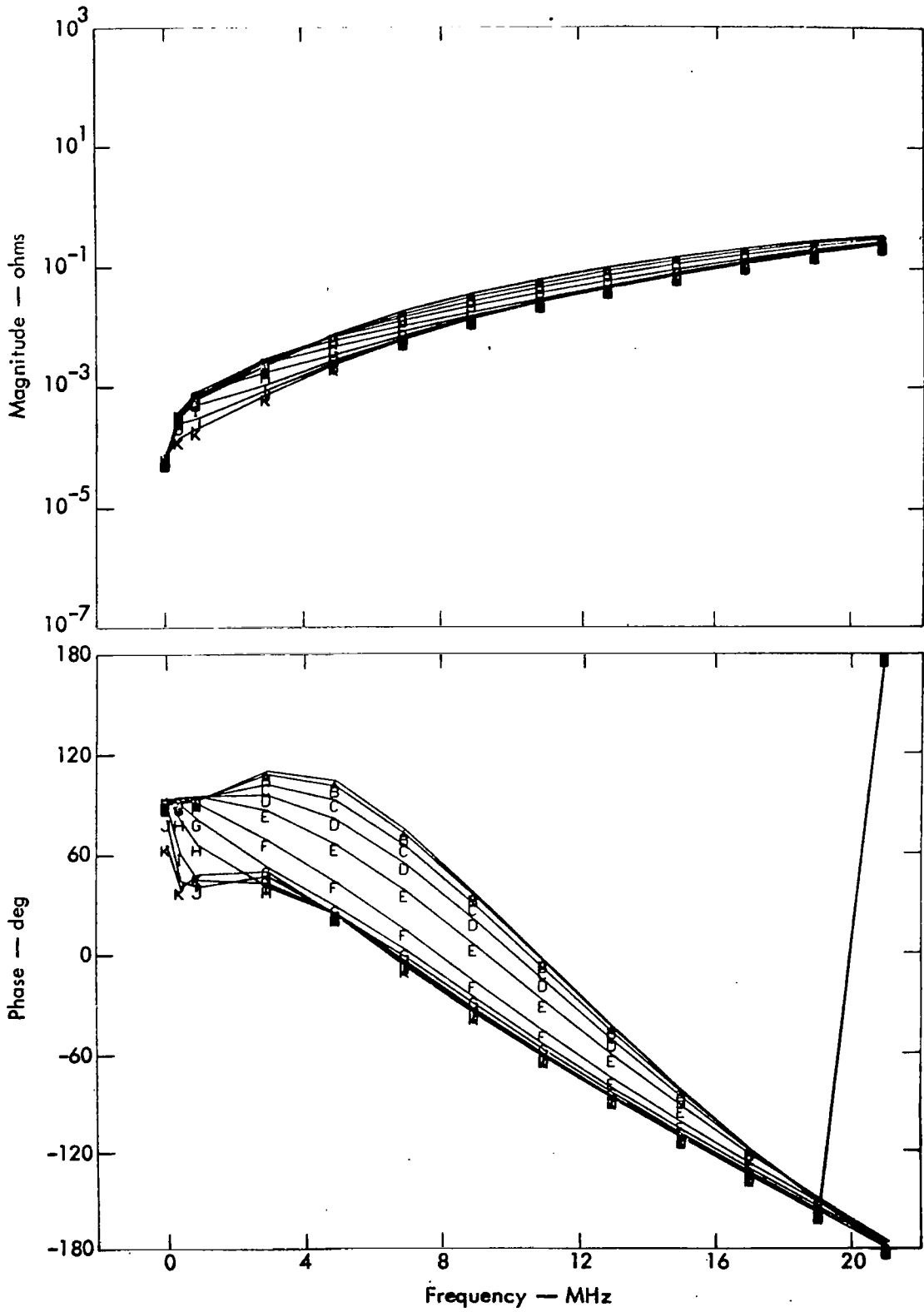


Fig. 27. Coplanar mutual impedance:  $\epsilon_r = 5$ ,  $d = 10$ .

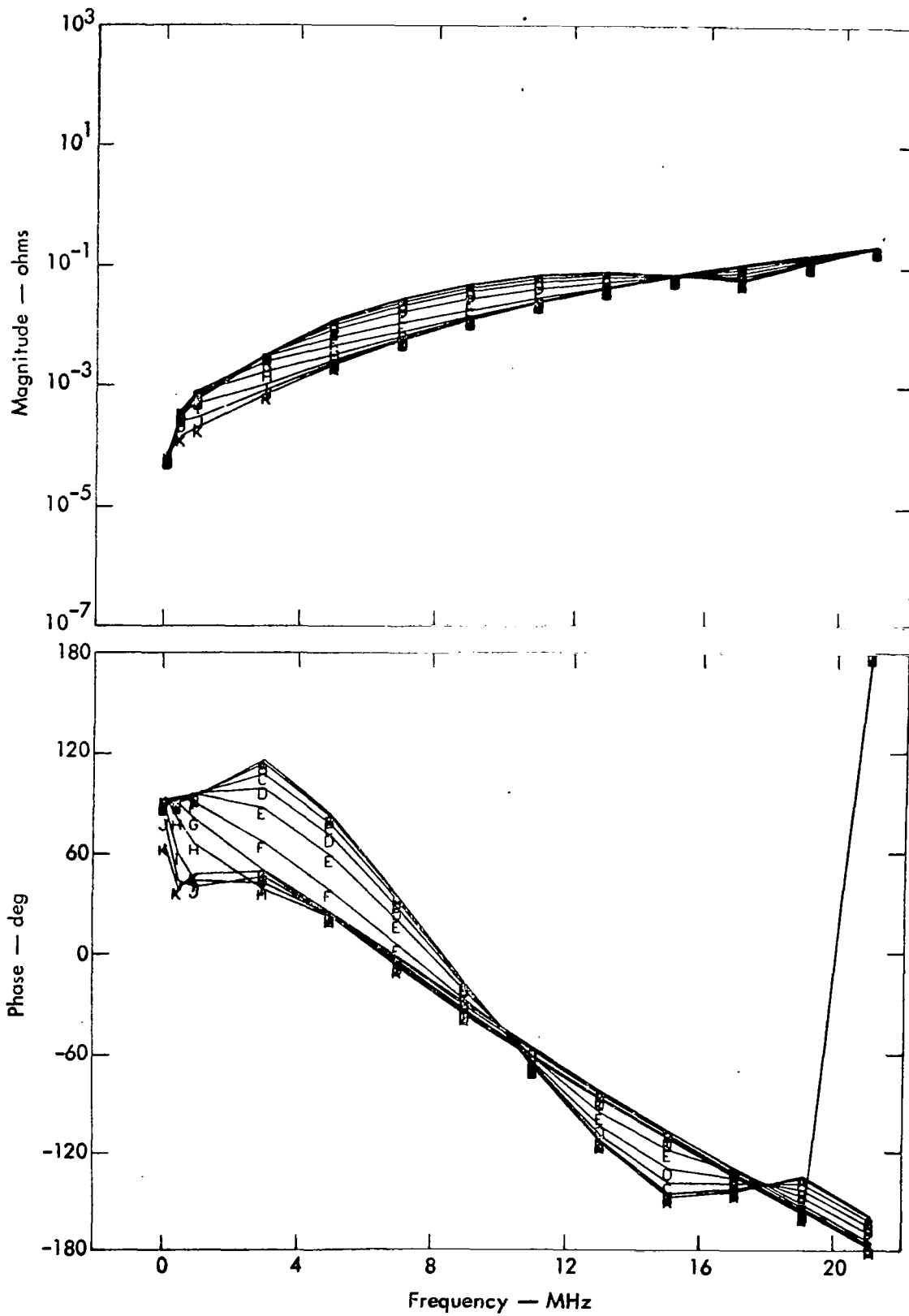


Fig. 28. Coplanar mutual impedance:  $\epsilon_r = 10$ ,  $d = 10$ .

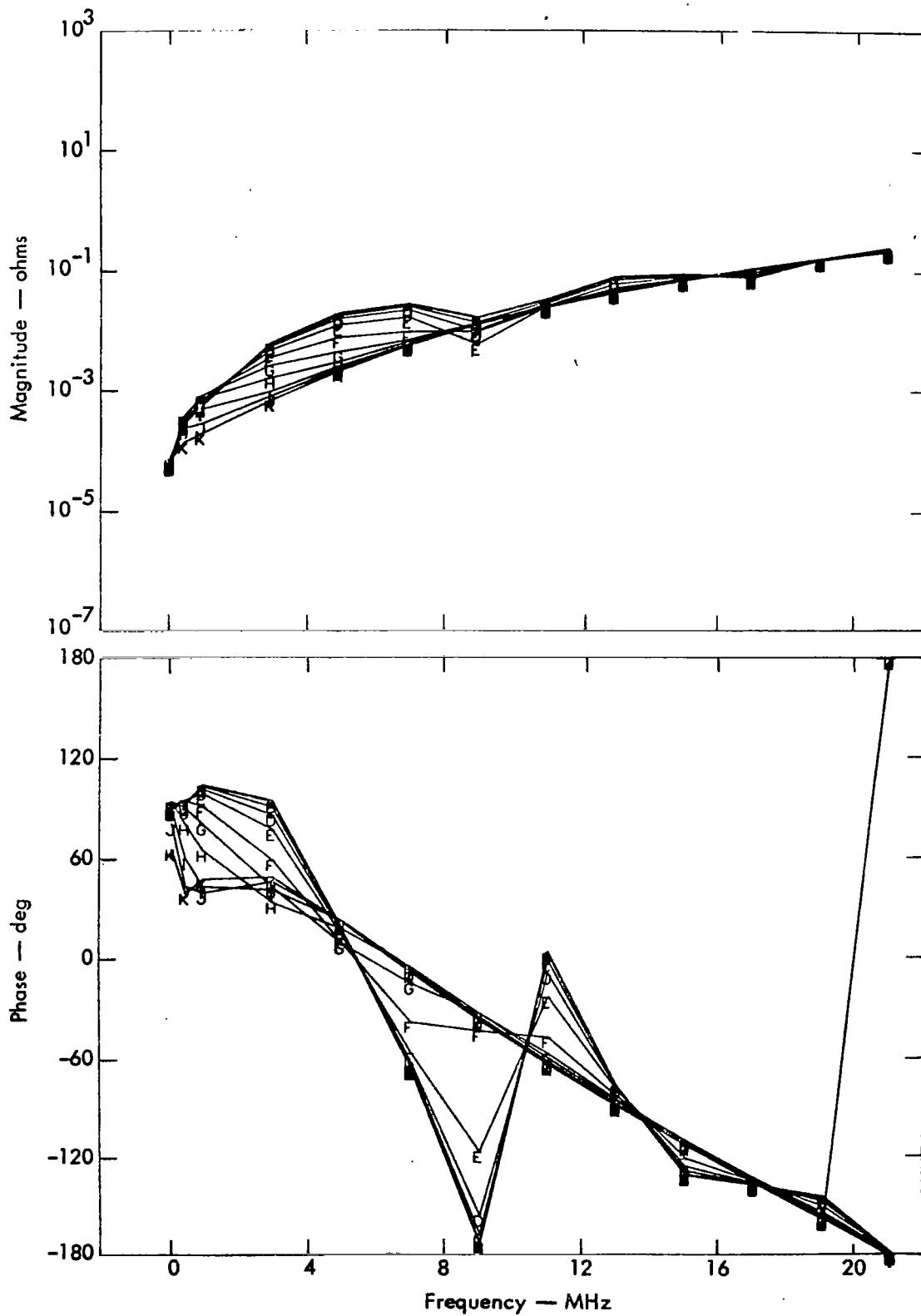


Fig. 29. Coplanar mutual impedance:  $\epsilon_r = 25$ ,  $d = 10$ .

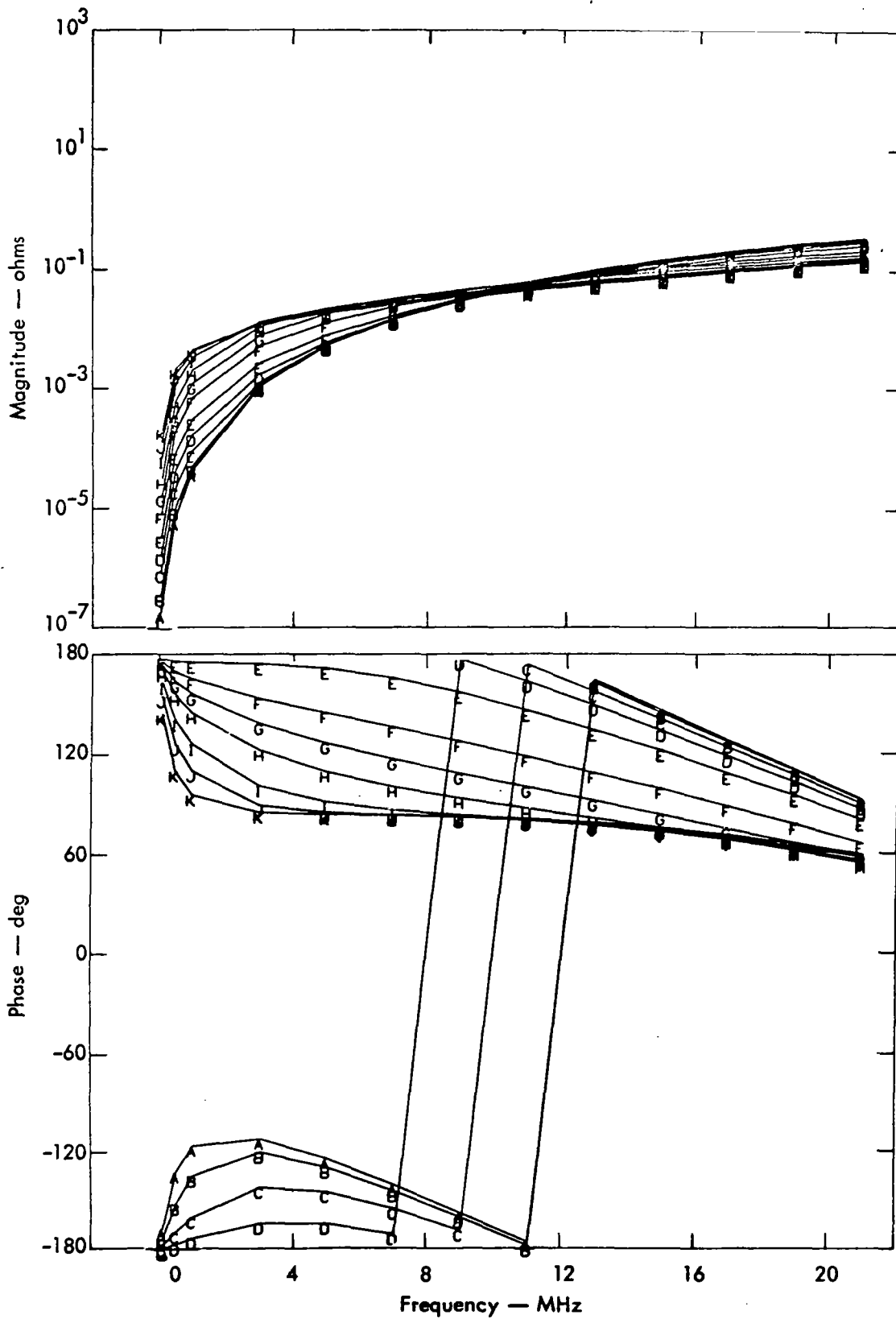


Fig. 30. Perpendicular mutual impedance:  $\epsilon_r = 5$ ,  $d = 5$ .

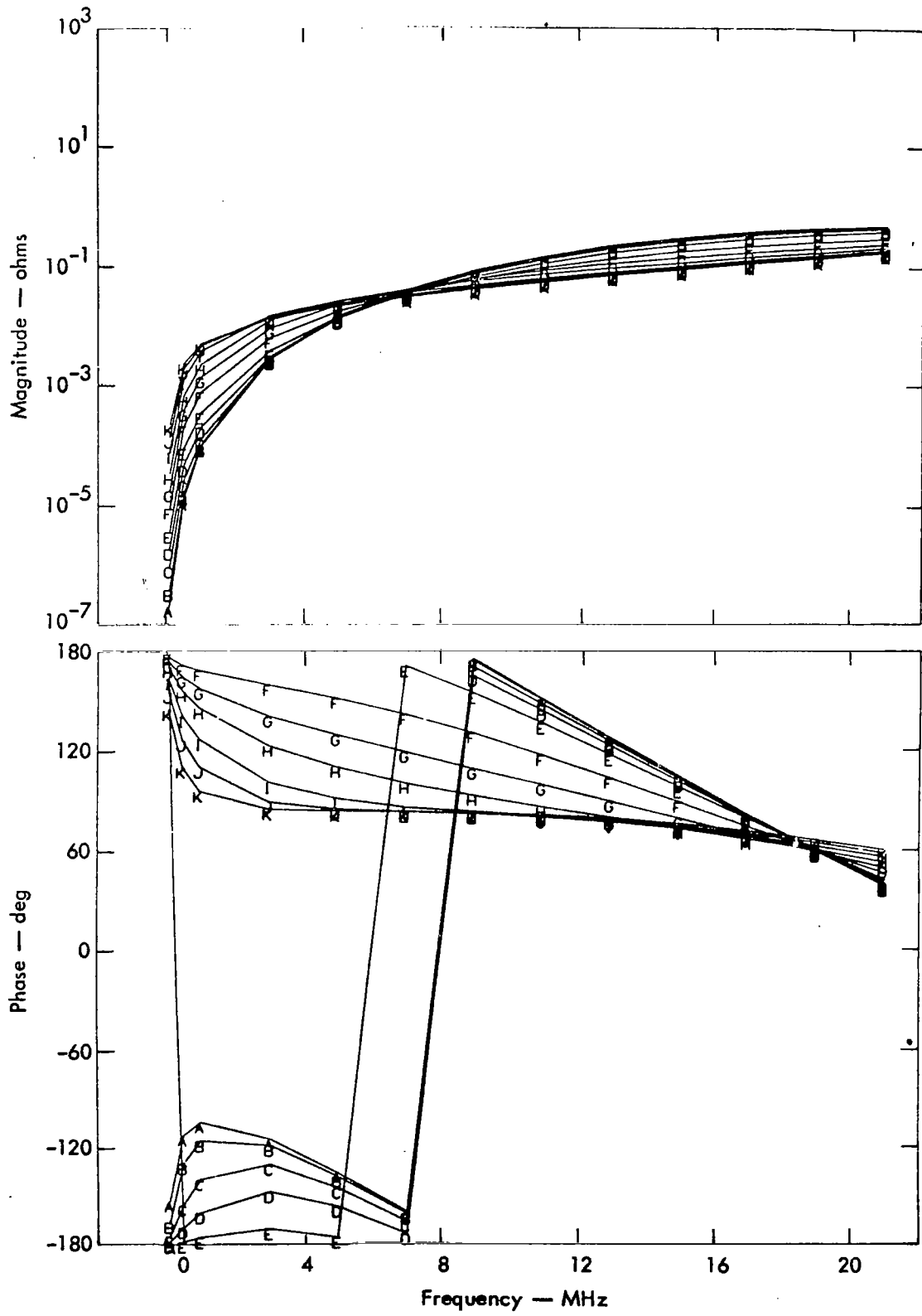


Fig. 31. Perpendicular mutual impedance:  $\epsilon_r = 10$ ,  $d = 5$ .

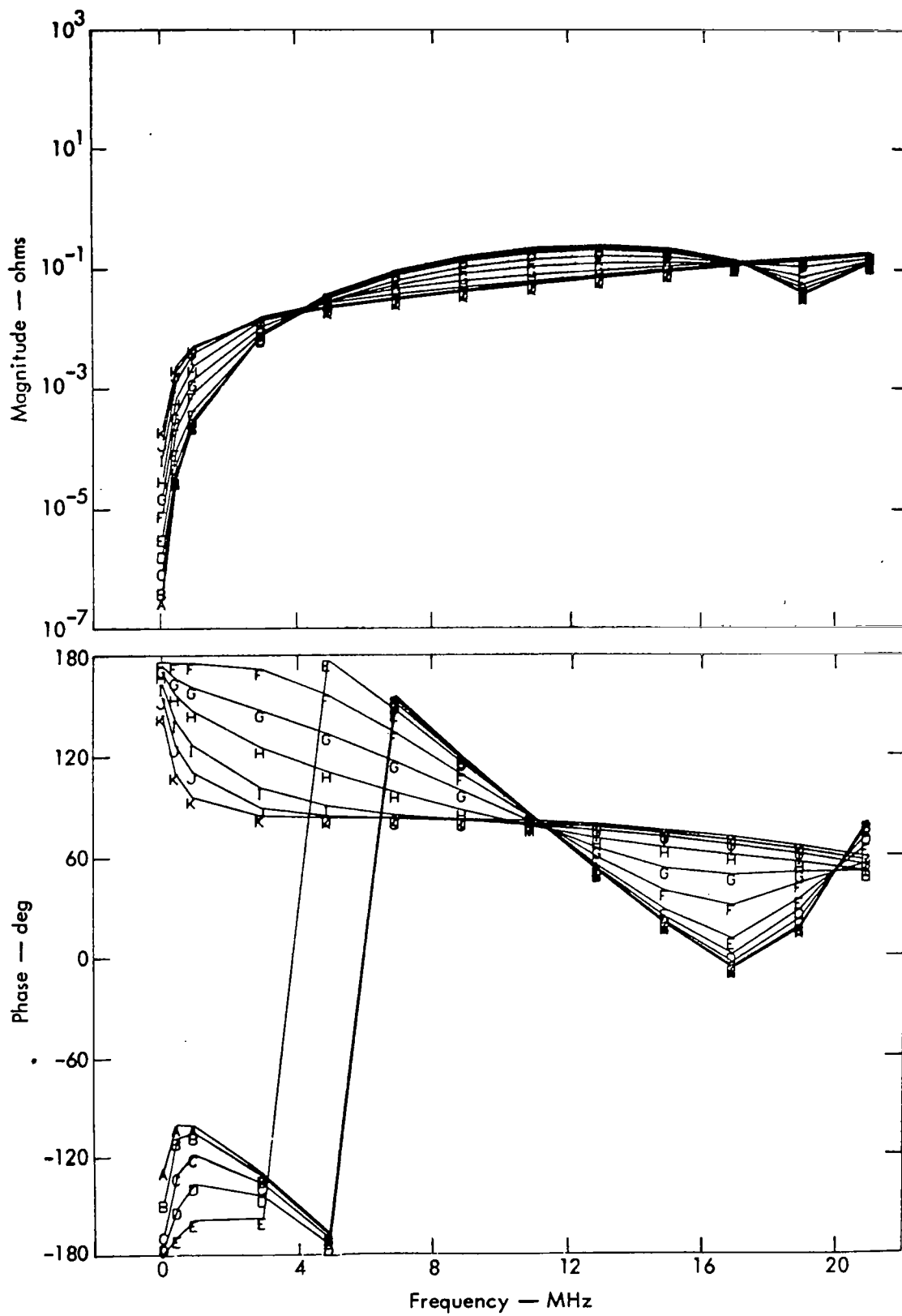


Fig. 32. Perpendicular mutual impedance:  $\epsilon_r = 25$ ,  $d = 5$ .

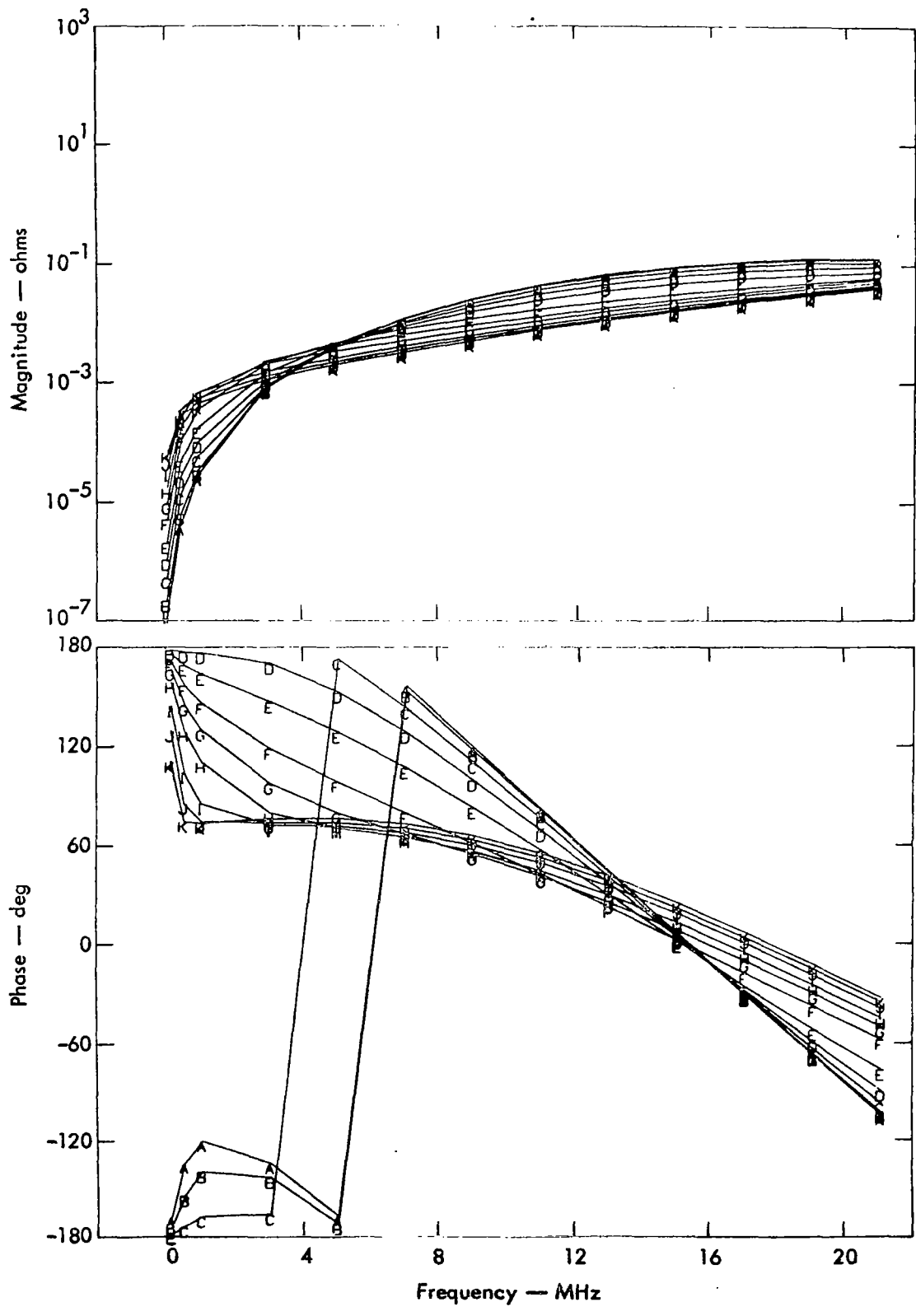


Fig. 33. Perpendicular mutual impedance:  $\epsilon_r = 5$ ,  $d = 10$ .

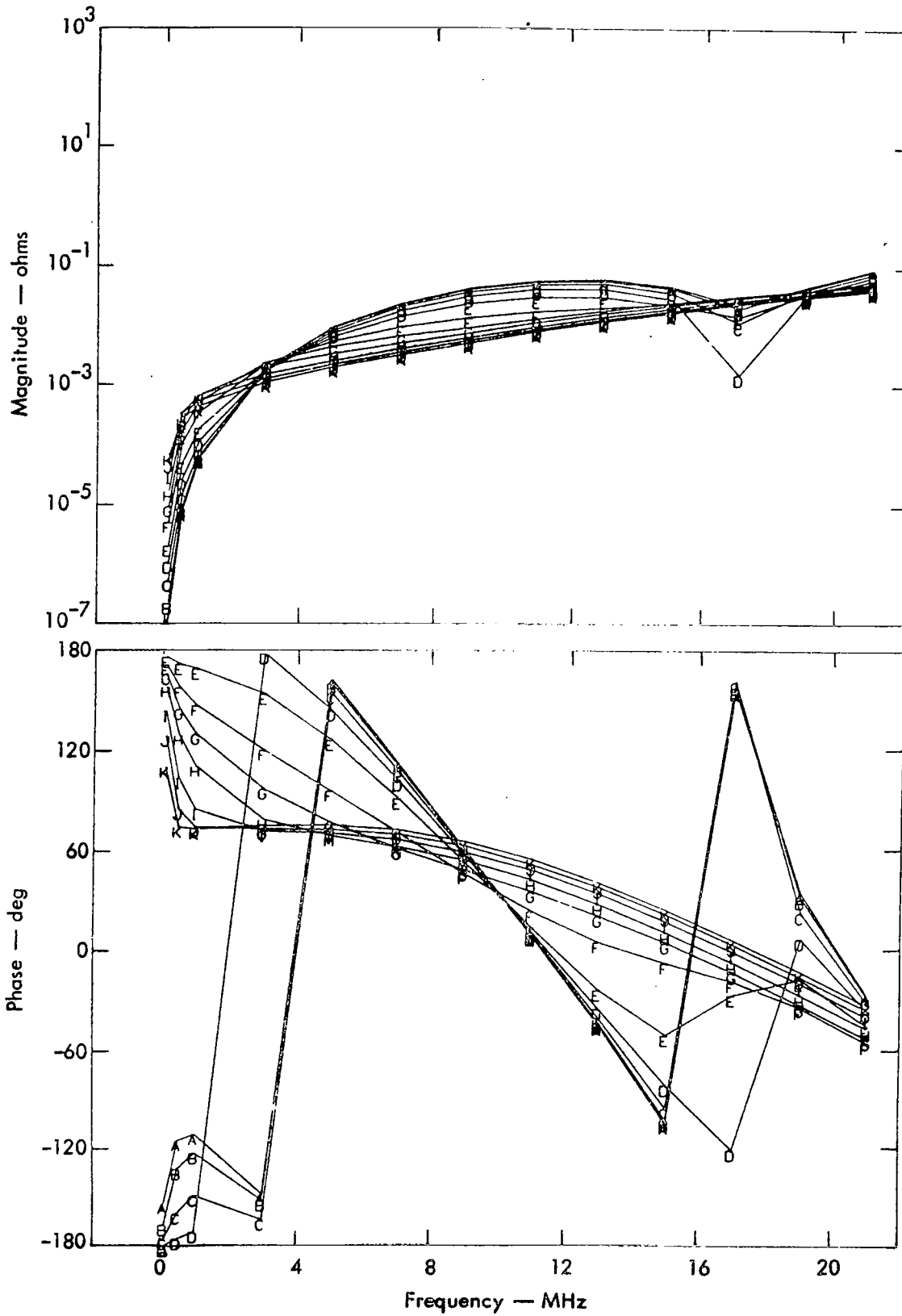


Fig. 34. Perpendicular mutual impedance:  $\epsilon_r = 10$ ,  $d = 10$ .

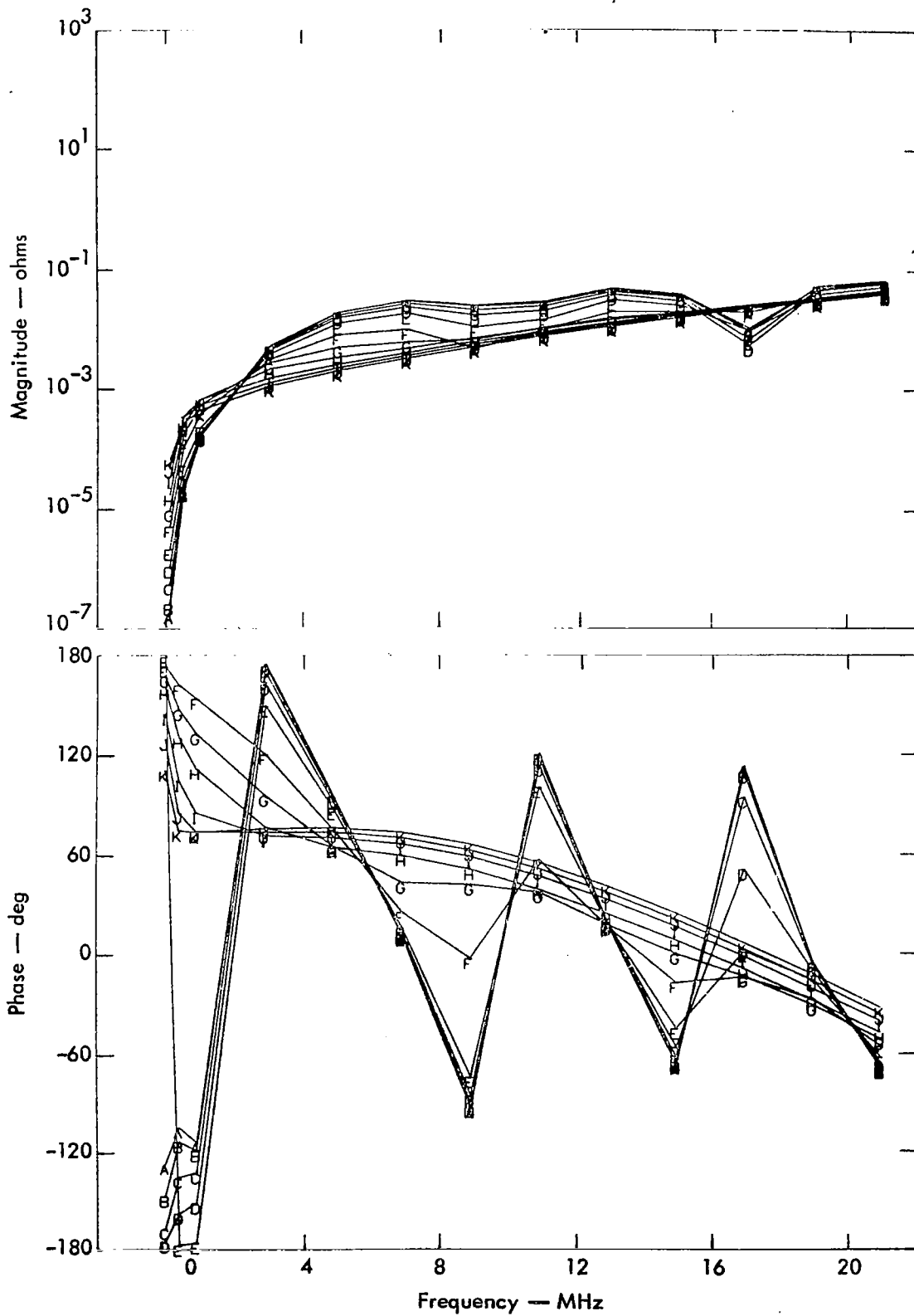


Fig. 35. Perpendicular mutual impedance:  $\epsilon_r = 25$ ,  $d = 10$ .

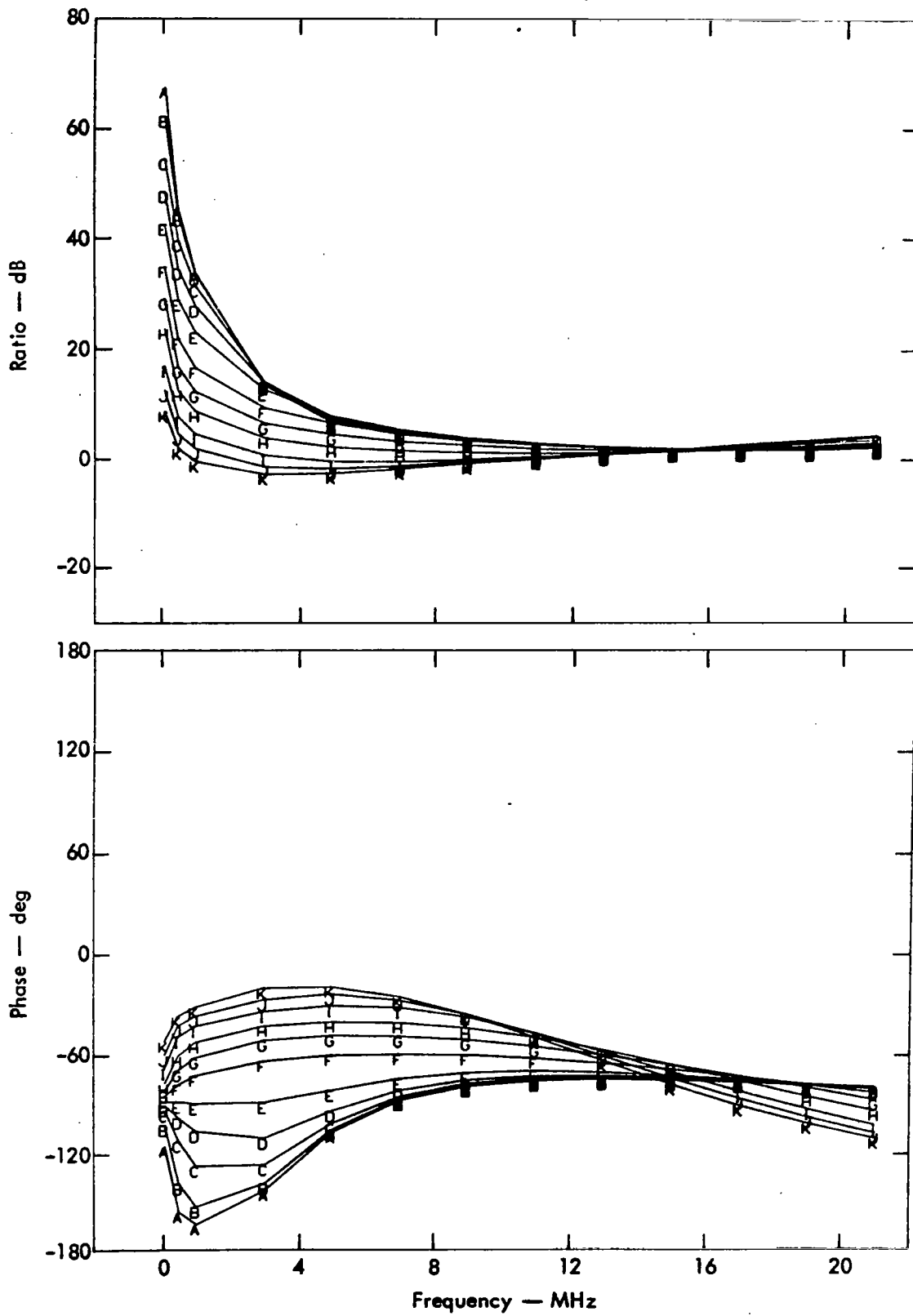
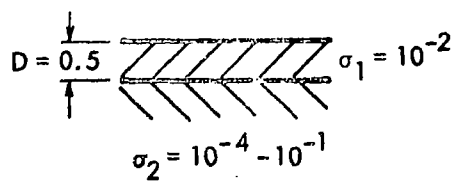
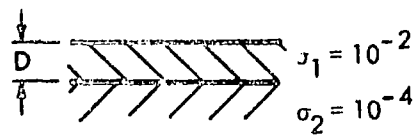


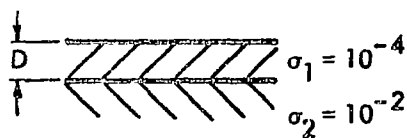
Fig. 36. Coplanar/perpendicular mutual impedances  $\epsilon_r = 10$ ,  $d = 5$ .



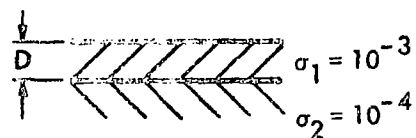
(a)



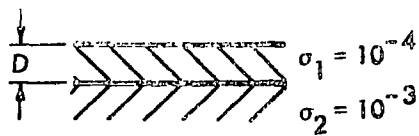
(b)



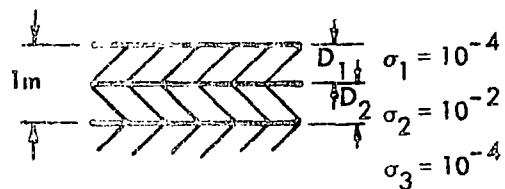
(c)



(d)



(e)



(f)

Fig. 37. Stratified media cases considered in this report.

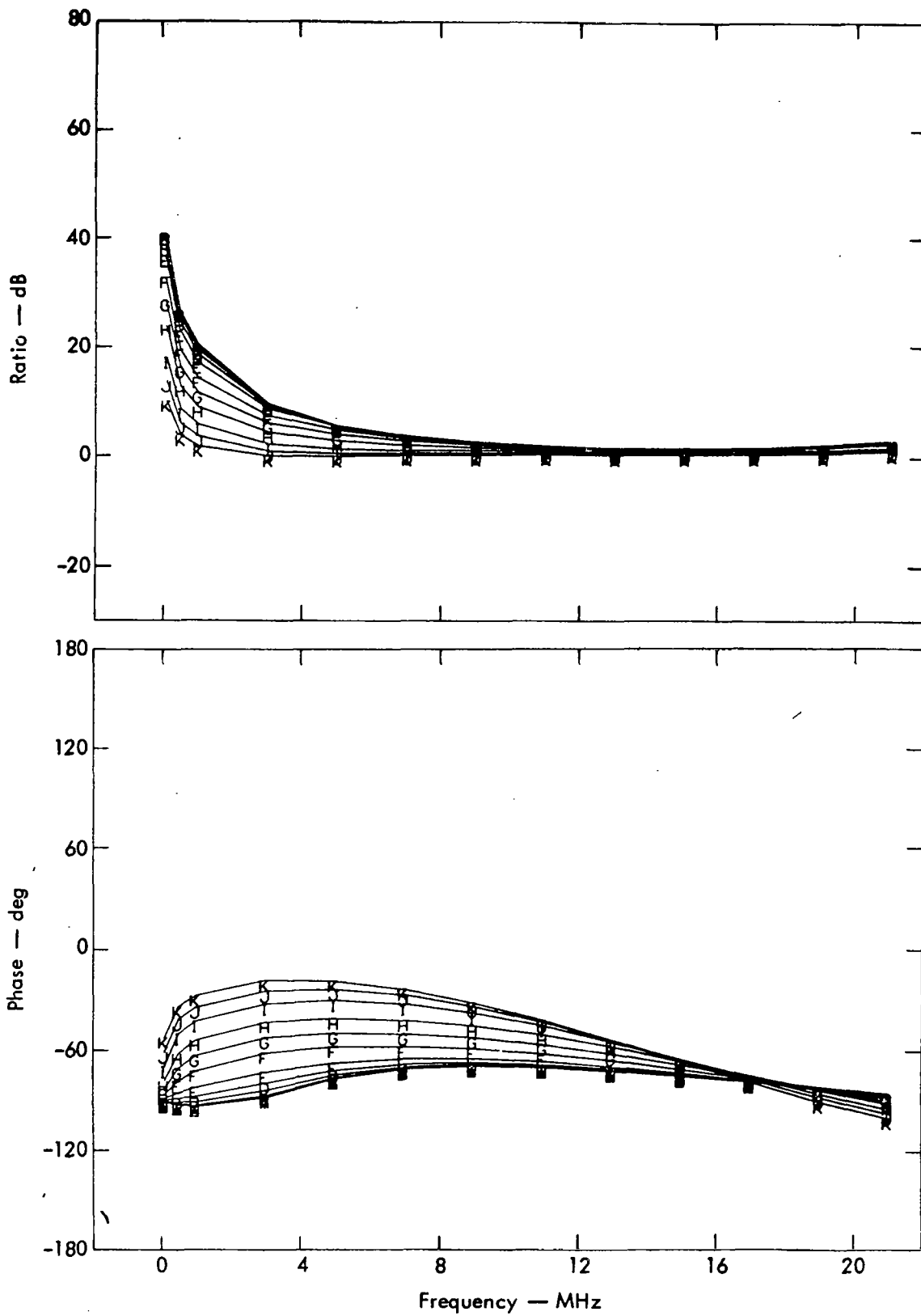


Fig. 38. Coplanar/perpendicular results for the situation depicted in Fig. 37a.

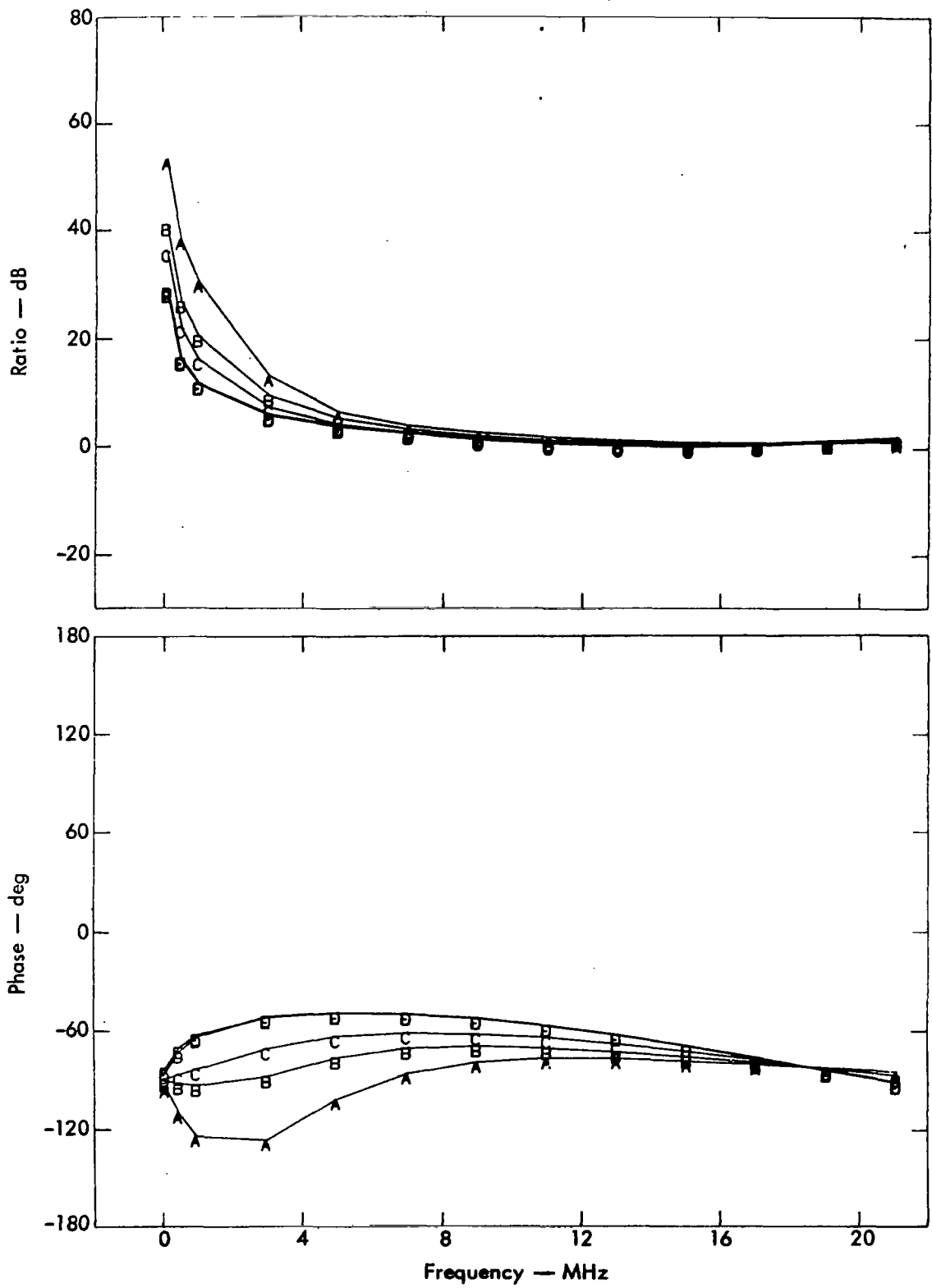


Fig. 39. Coplanar/perpendicular results for the situation depicted in Fig. 37b.

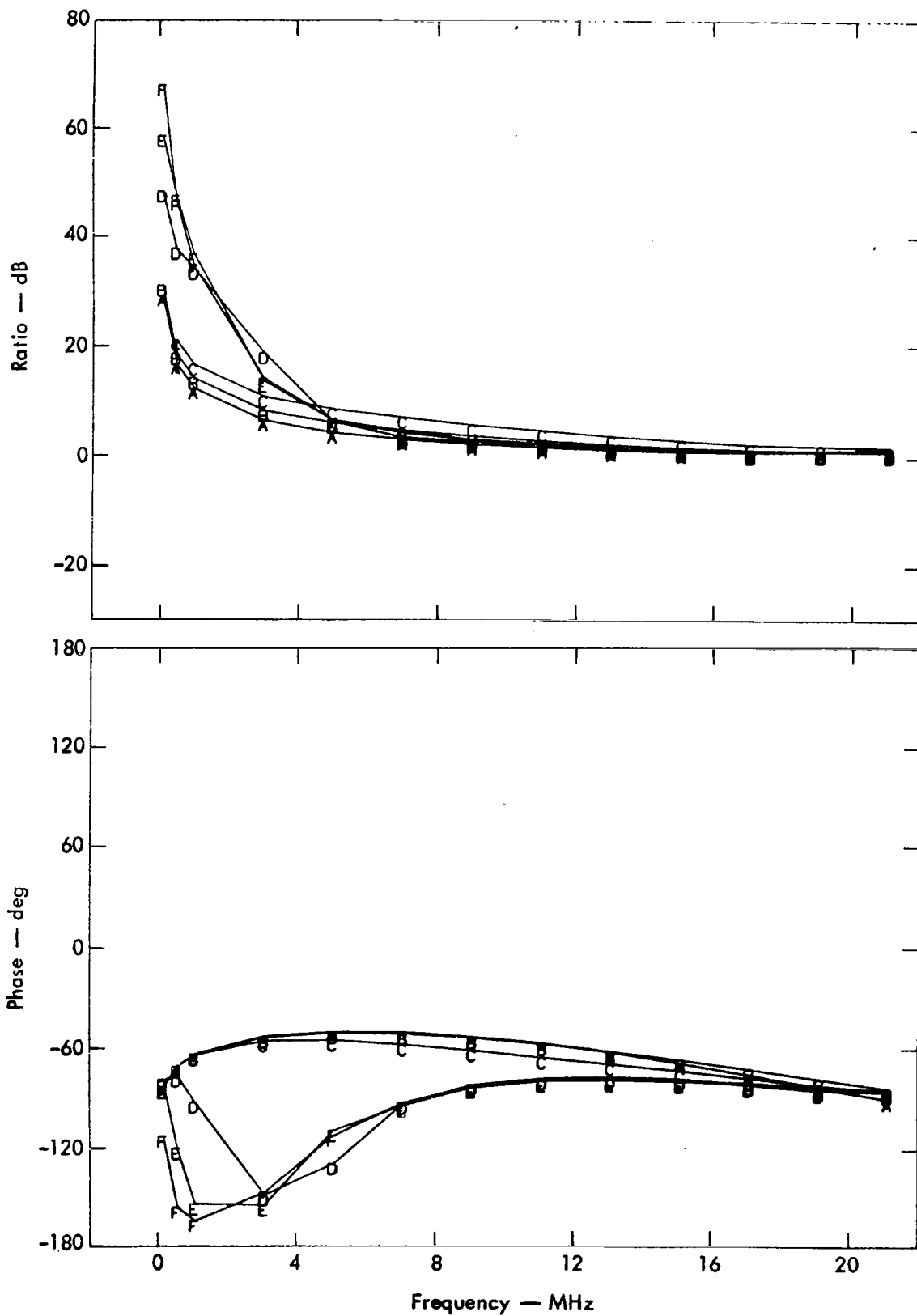


Fig. 40. Coplanar/perpendicular results for the situation depicted in Fig. 37c.

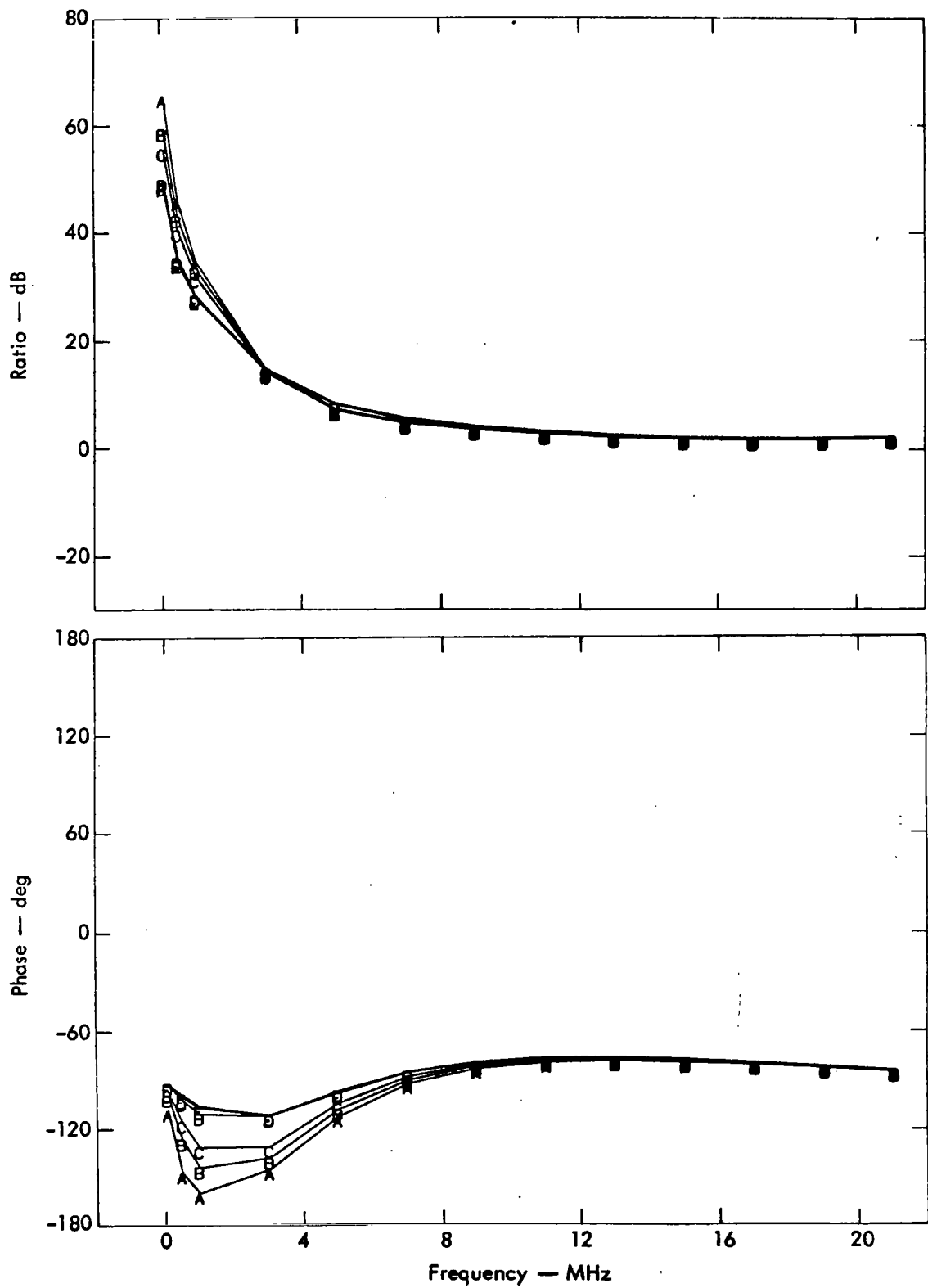


Fig. 41. Coplanar/perpendicular results for the situation depicted in Fig. 37d.

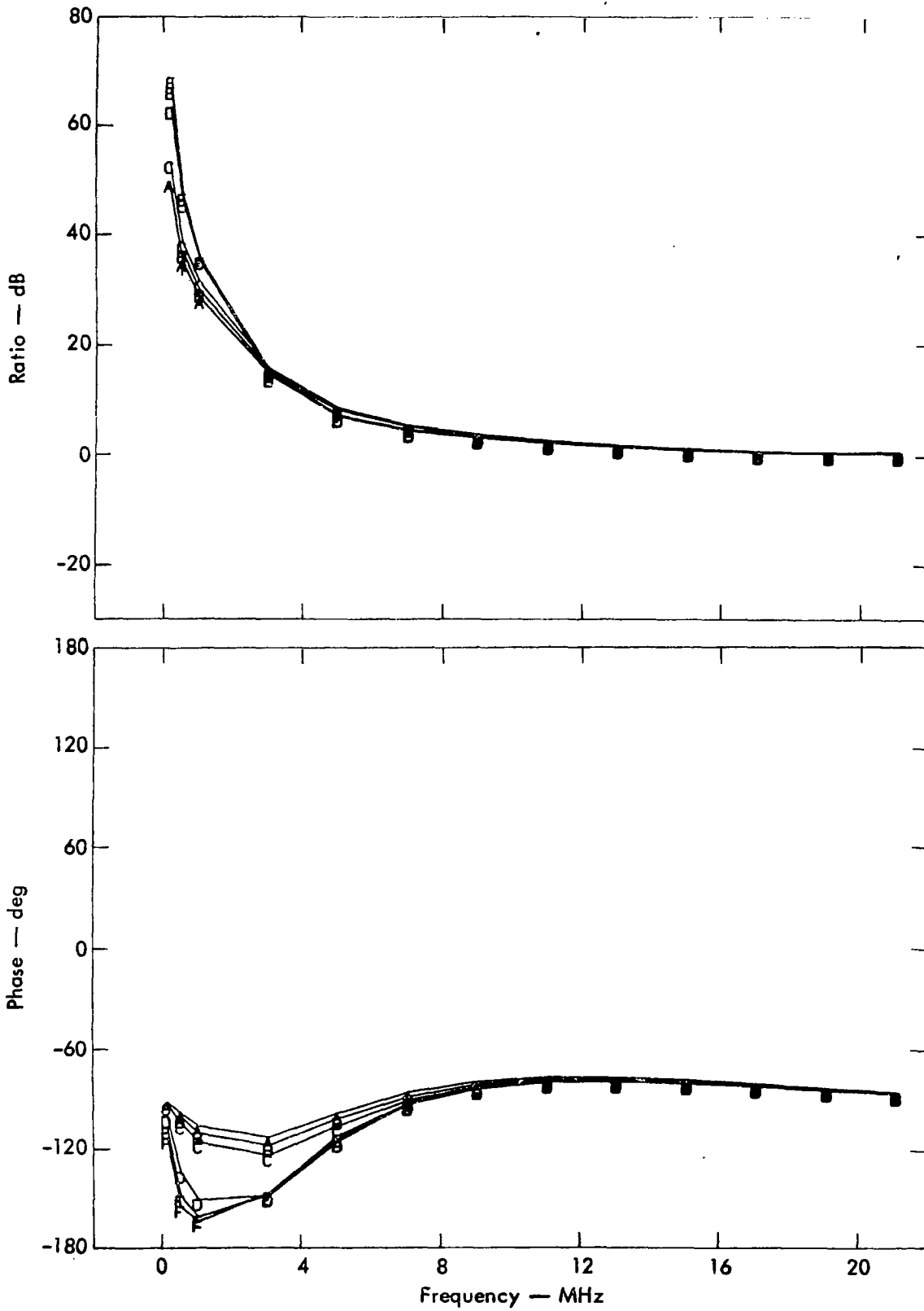


Fig. 42. Coplanar/perpendicular results for the situation depicted in Fig. 37e.

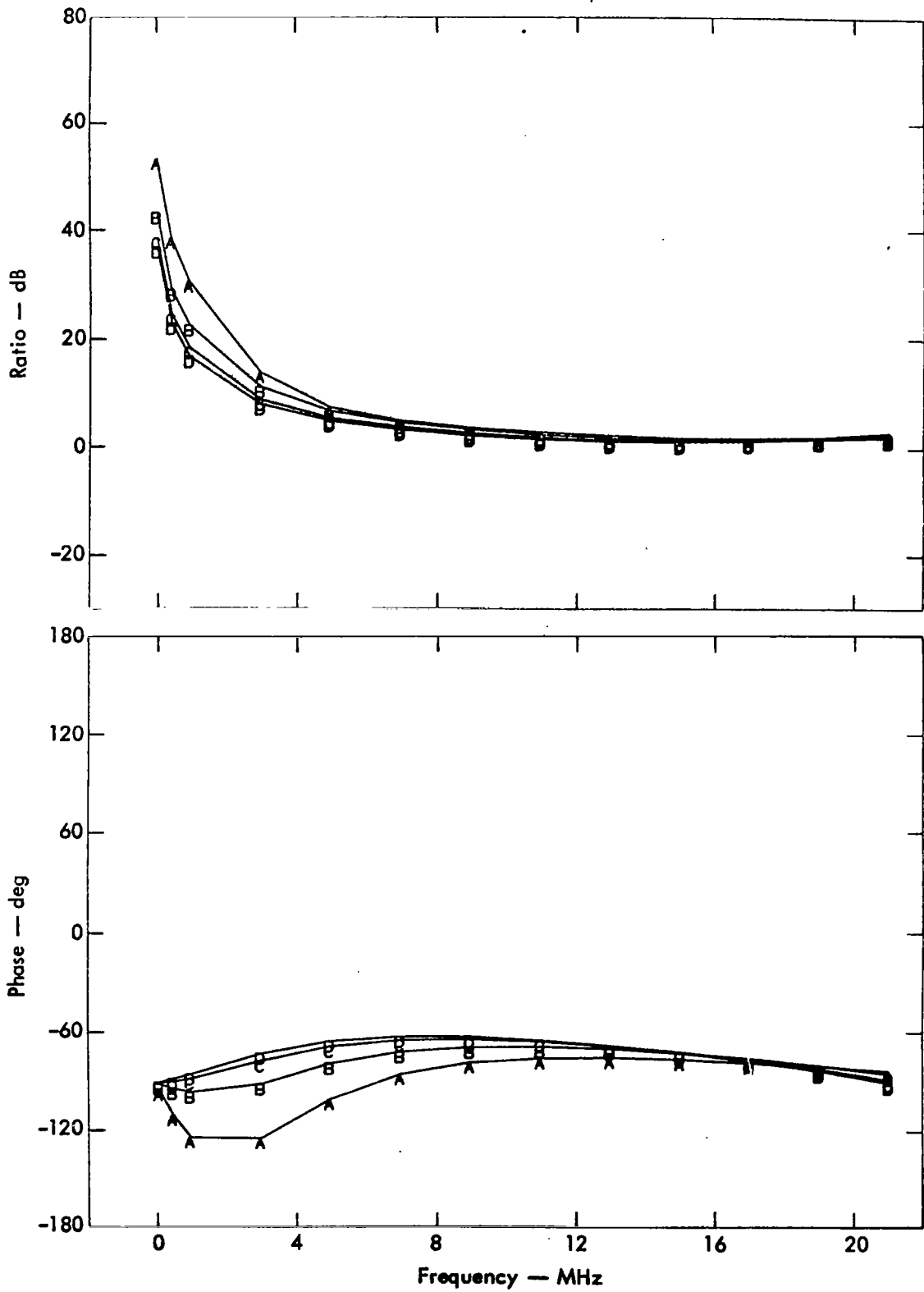


Fig. 43. Coplanar/perpendicular results for the situation depicted in Fig. 37f.

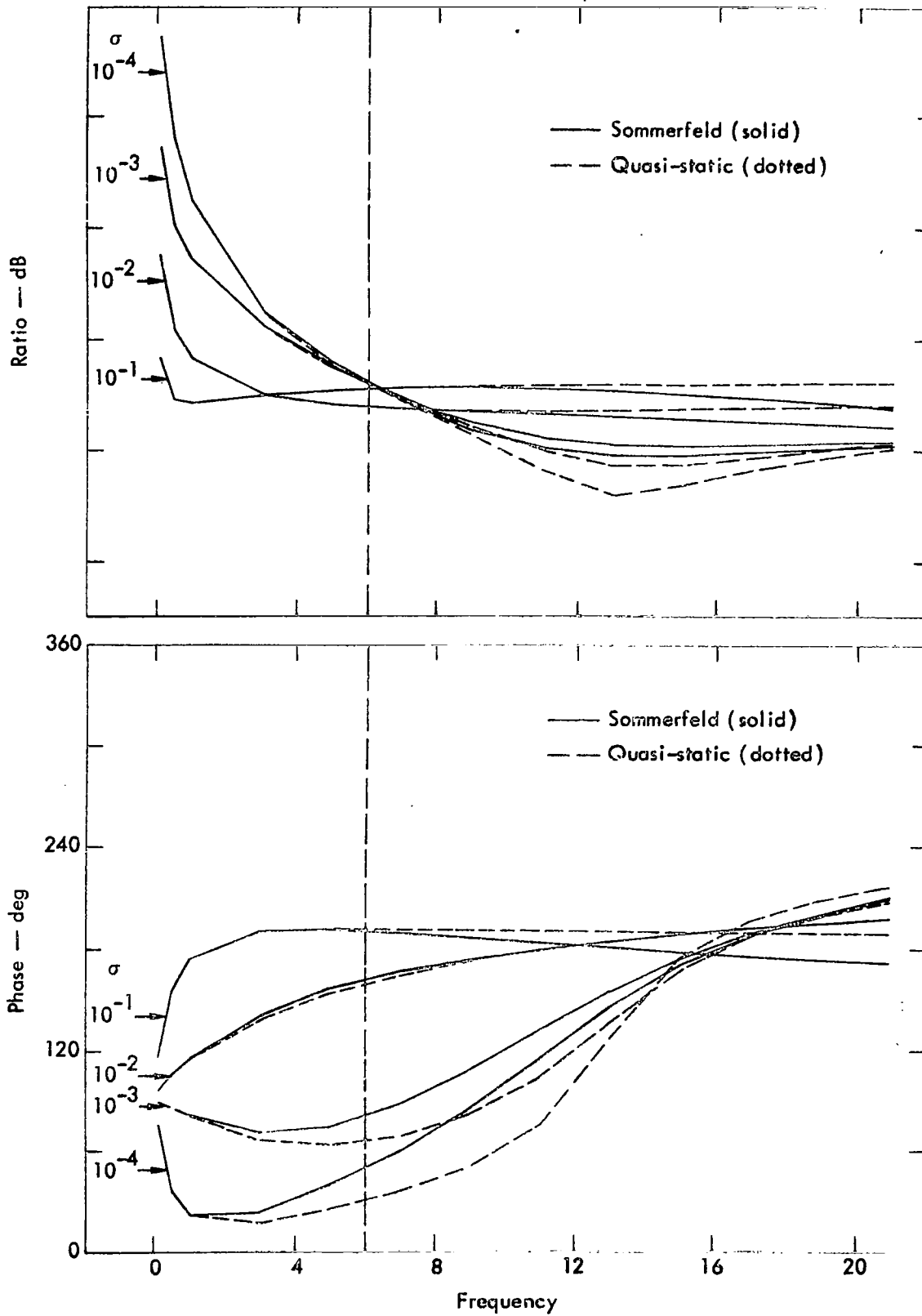


Fig. 44. Comparison of Sommerfeld evaluation and quasistatic approximation results for the coaxial/perpendicular situation of  $\epsilon_r = 5$  and  $d = 5$  m.

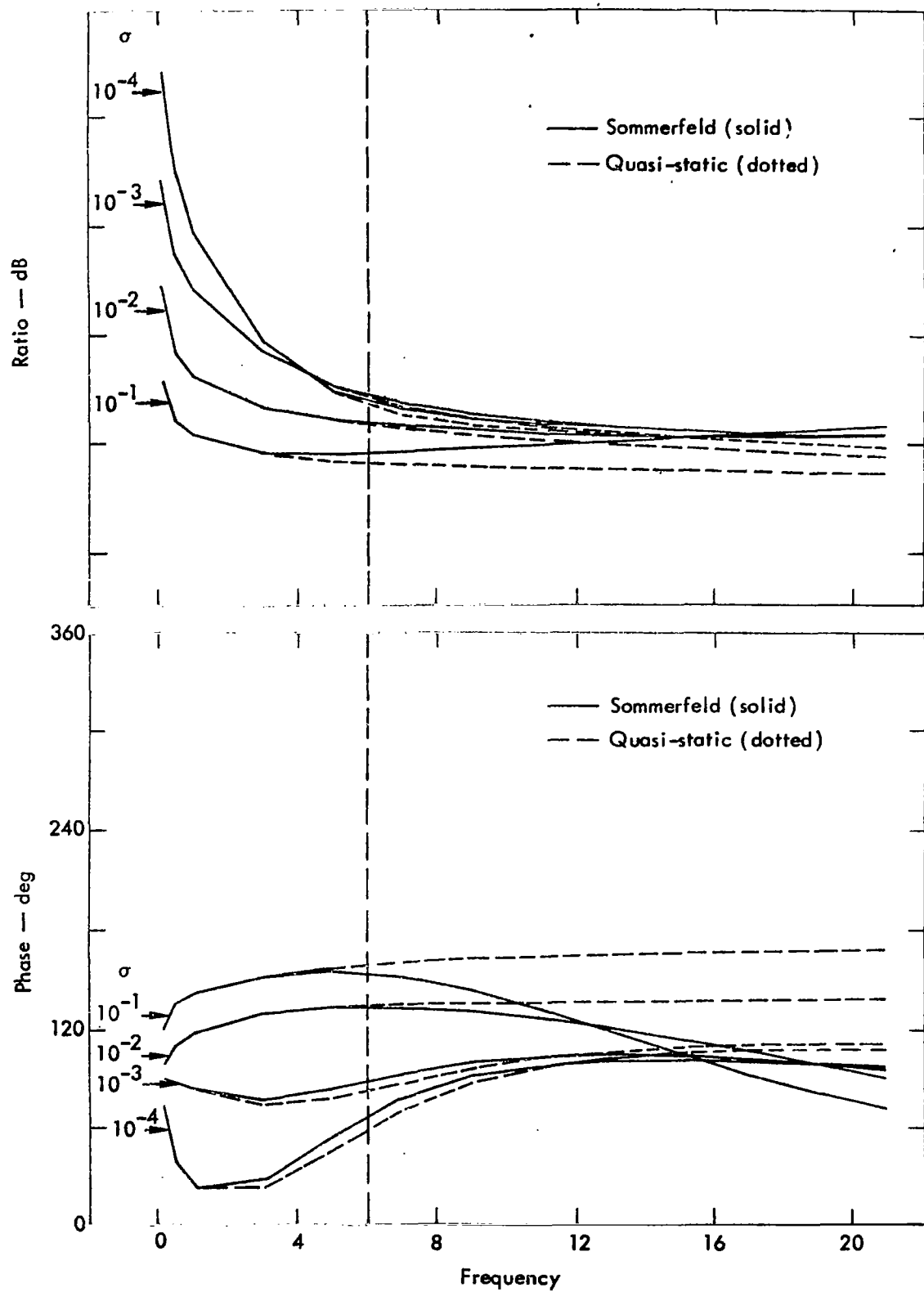


Fig. 45. Comparison of Sommerfeld evaluation and quasistatic approximation results for the coplanar/perpendicular situation of  $\epsilon_r = 5$  and  $d = 5$  m.

## ACKNOWLEDGMENTS

The research described in this report was accomplished under sponsorship of the Advanced Research Projects Agency, with the work monitored by Col. John K. Lerohl. A critical reading and numerous helpful comments were graciously provided by Myron W. Knapp.

Numerous experimental refinements were suggested by Carl Wallace and Ray Egbert.

## REFERENCES

1. G. V. Keller and F. C. Frischknecht, Electrical Methods in Geophysical Prospecting (Pergamon Press, New York, 1970).
2. A. Sommerfeld, "Uber die Ausbreitung der Wellen in der Drahtlosen Telegraphie," Ann, Physik, 88, No. 2, 665 (1909)
3. J. R. Wait, "Mutual Coupling of Loops Lying on the Ground", Geophysics XIX, 290 (1954).
4. J. R. Wait, "Mutual Electromagnetic Coupling of Loops Over Homogeneous Ground," Geophysics XX, 630 (1955).
5. J. R. Wait, "Induction by an Oscillating Magnetic Dipole Over a Two Layer Ground," Applied Scientific Research, Sect. B, pp. 73-80 (1957).
6. J. R. Jöhler, ESSA Technical Report, ERL 122-ITS 86 (1969).
7. E. C. Barrows, private communication.

## REFERENCES

8. E. C. Barrows, R. H. Espeland and B. Wieder. "Measurements of Ground Conductivity Using the Two-Loop Technique in the Frequency Range 50 - 150 kHz," paper presented at 1971 IEEE G-AP Intern. Symp., UCLA, Los Angeles, California.
9. K. P. Spies and J. R. Wait, "Determining Electrical Ground Constants from the Mutual Impedance of Small Coplanar Loops," IEEE Trans. Antennas & Propagation AP-20, 501 (1972).
10. R. H. Ott and J. R. Wait, "The Transient Response of a Magnetic Dipole Over a 2-layer Ground in the Quasi-Static Regime," paper presented at 1971 IEEE G-AP Intern. Symp., UCLA, Los Angeles, California.
11. J. R. Wait, Electromagnetic Waves in Stratified Media (Pergamon Press, New York, 1970).
12. S. H. Ward, "Electromagnetic Sounding Over Inhomogeneous Terrains," paper presented at 1971 IEEE G-AP Intern. Symp., UCLA, Los Angeles, California.
13. E. K. Miller, A. J. Poggio, G. J. Burke and E. S. Selden, "Analysis of Wire Antennae in the Presence of a Conducting Half Space: Part I. The Vertical Antenna in Free Space; Part II. The Horizontal Antenna in Free Space," to be published in the Canadian Journal of Physics.